

1           **Projected climate change impacts for Chesapeake Bay**

2

3                           **Victoria J. Coles<sup>1</sup> and David G. Kimmel<sup>1,2</sup>**

4       <sup>1</sup>: University of Maryland Center for Environmental Science, Horn Point Laboratory, PO

5       Box 775, Cambridge, MD 21613

6

7       <sup>2</sup>: Now at: Department of Biology and Institute for Coastal Science and Policy, East

8       Carolina University, Greenville, NC 27858, United States

9

10   **Draft June 25, 2008**

11   **For submission to:**

12   **Climate Research**

13

1 **ABSTRACT:**

2 The World Climate Research Programme's Coupled Model Intercomparison Project  
3 model ensemble (Meehl et al. 2007) for two high and lower emissions scenarios is used  
4 to estimate future climate relevant to the physics and ecology of Chesapeake Bay.  
5 Individual model error for local temperature and precipitation metrics is is calculated, and  
6 the mean model is is found to represent present day climate better than any single model  
7 for these small regional scales. Average air temperature is projected to warm by 2.5-4.5C,  
8 and this is much higher than the present day interannual variability in air temperature.  
9 The mean model also projects higher precipitation in winter, but the changes are well  
10 within the present day interannual variability. Indices of extreme events are also  
11 evaluated with climate projected to become more variable in general with more intense  
12 precipitation events, fewer long-term droughts and more extensive heatwaves (the longest  
13 period with consecutive days above the 20<sup>th</sup> century 95<sup>th</sup> percentile daily maximum  
14 temperature). These changes imply greater freshwater and nutrient inputs into  
15 Chesapeake Bay leading to prolonged water column stratification, increased prevalence  
16 of hypoxia and larger temperature fluctuations in shallow regions.

17

18 **Key words:**

19 regional climate forecast, Chesapeake Bay, multi model

1  
2  
3  
4  
5  
6  
7  
8  
9  
10  
11  
12  
13  
14  
15  
16  
17  
18  
19  
20  
21  
22  
23

1. INTRODUCTION

The recent release of the Intergovernmental Panel on Climate Change’s (IPCC) Fourth Assessment Report: Climate Change 2007 (AR4) shows unambiguously that anthropogenic release of a suite of greenhouse gasses is warming the globe. The assessment consists of a review of the literature on observational and paleo-based evidence for climate variations in the past and present and an assessment of projections from different global Atmosphere Ocean coupled General Circulation Model (AOGCM) simulations. Each AOGCM was run for a number of equally possible future emissions scenarios based on the IPCC Special Report on Emissions Scenarios (SRES). Together, these model simulations represent the state of the art projection for future climate at the global scale.

Ideally, a large number of regional climate models, or a single regional climate model forced by an ensemble of global climate models, would be used to project future climate changes at the scale of the Chesapeake Bay watershed. Either approach would incorporate local processes that may influence climate, while using the ensemble forecasting approach. However at present no such ensemble exists over any region of North America (Christensen et al. 2007). Therefore, this study provisionally uses the existing AR4 model simulations to make projections for future climate forcing of Chesapeake Bay conditions. The regionally averaged projections are available online at <http://www.hpl.umces.edu/vcoles/cbayclim.htm>.

1 The AR4 report (Christensen et al. 2007) includes information on regional climate  
2 change based on an analysis of the submitted AOGCMs. General themes that emerged  
3 relevant to the eastern North Atlantic included: a general shift to atmospheric conditions  
4 somewhat representative of the positive phase of the North Atlantic Oscillation (NAO),  
5 including poleward expansion of the subtropical high, leading to the poleward migration  
6 of the winter stormtrack. Over the eastern North Atlantic continent (defined in their study  
7 as 25°N-50°N, 85°W-50°W), median temperature and precipitation changes from the end  
8 of the 20<sup>th</sup> century to the end of the 21<sup>st</sup> century were reported as +3.6°C and +7%  
9 respectively. The frequency of extreme warm, wet or dry conditions was also reported,  
10 based on a criterion that uses the warmest, wettest, and driest year in the last 20 years of  
11 the 20<sup>th</sup> century (the top 5%) as the measure of extreme conditions. In the eastern North  
12 Atlantic warmest and wettest extreme conditions are projected to occur 100 and 29% of  
13 the time respectively over the period 2080-2099. Because the region of the Chesapeake  
14 Bay watershed is much smaller (roughly 35°N-43°N, 84°W-75.5°W as defined in our  
15 study; Figure 1), this study assesses whether these general themes hold true, and also the  
16 intervening time periods between 2000 and 2100 that are more relevant to present day  
17 management concerns.

18

19 Climate change is explicitly mentioned in the historic Bay 2000 agreement between the  
20 states of Maryland, Pennsylvania, Virginia, the District of Columbia, the Chesapeake Bay  
21 commission, and the United States Environmental Protection Agency. However relatively  
22 little work has been done on integrating climate change into management decisions  
23 relating to the protection and restoration of the Chesapeake Bay. This study is motivated

1 by the establishment of the Maryland Commission on Climate Change, which was tasked  
2 with providing a comprehensive climate change impact assessment over a period of 9  
3 months. The aim is to provide a preliminary estimation of potential future climate over  
4 the Chesapeake Bay watershed. Three future time points were chosen: 2025, 2050, and  
5 2100 to provide short, medium and long-term projections. The consequences of these  
6 projections on Chesapeake Bay are discussed with emphasis on shifts in the physical and  
7 biogeochemical dynamics of Chesapeake Bay. In particular, we focus on properties of the  
8 climate system such as surface air temperature, precipitation, snow cover, sea level rise,  
9 and indices of extreme temperature and precipitation.

10

## 11 **2. METHODS**

### 12 **2.1. Global models**

13 This study draws on a subset of the models archived at the Program for Climate Model  
14 Diagnosis and Intercomparison (PCMDI) as part of the World Climate Research  
15 Programme's (WCRP) Coupled Model Intercomparison Project (CMIP3) multi-model  
16 dataset. We have not used statistical downscaling techniques (e.g. (Crane and Hewitson  
17 1998; Hayhoe et al. 2007; Wilby et al. 2004). Our approach is to use a large model  
18 ensemble to estimate spatially averaged changes over the region encompassing the  
19 Chesapeake Bay watershed, and to include a large number of diagnostic variables. This  
20 allows the individual user to apply these anomalies to local weather patterns. The results  
21 are very similar for equivalent variables to the larger scale analysis in the IPCC report  
22 (Christensen et al, 2007), and with the statistically downscaled analysis of Hayhoe et al,  
23 2007, indicating that while climate models should not be directly compared with local

1 weather patterns, the broader analysis of a regional average may be useful particularly  
2 when coupled with an understanding of the local spatial variability.

3

4 Metrics are constructed for evaluating individual model projections that include global, as  
5 well as local skill at representing 20<sup>th</sup> century climate. These metrics are used to evaluate  
6 which models should be retained in the study (Table 1). Four models (14, 22, 13, 10, see  
7 Table 1) are eliminated because a recent study (Reichler and Kim 2008), suggested that  
8 their performance based on a combination of global metrics was significantly poorer than  
9 the ensemble of models at large. The local metrics are focused on precipitation and  
10 temperature because observationally based timeseries are available over the majority of  
11 the 20<sup>th</sup> century, which allows for evaluation of the models over seasonal to decadal  
12 timescales. Monthly average model precipitation and surface air temperature are gridded  
13 to a common 0.5° resolution and then averaged spatially over the Chesapeake Bay  
14 watershed region. The temperature and precipitation climatologies generated at the  
15 Climate Research Unit of the University of East Anglia, UK are similarly regridded and  
16 averaged to ensure consistent spatial averages for the comparison (Hulme 1992; Hulme  
17 1994; New et al. 2002).

18

19 The model error score combines metrics for: mean temperature and precipitation, the  
20 error in model trend over the 20<sup>th</sup> century, the error in seasonal and 10 year boxcar  
21 filtered correlations, and the model – data error in standard deviation of the full and  
22 filtered timeseries. Models with worse than average global skill are also penalized. To  
23 highlight model differences, the errors are normalized to the ensemble range of error for

1 each individual metric. Thus each error ranges from 0 for the best performing model, to 1  
2 for the worst performing model.

3

4 The final equation for model error (Equation 1) is

$$ME = \sum w_j \varepsilon_j \quad (1)$$

5

6 Individual model error scores are illustrated in Figure 2a. Despite the normalization, there  
7 are not large differences in the total error between the models. In analyses by Achuta-Rao  
8 et al. 2006, the mean model, a simple average across all different AOGCM's that were  
9 run using the same external forcing conditions, provided a better estimate of present  
10 climate than any individual model. Here, the regional mean model has the lowest error  
11 score of any individual model (Fig 2a), indicating that this global result holds at small  
12 scales also, that uncorrelated model errors are being removed in the averaging process,  
13 and these errors represent a significant fraction of the total model error. This study  
14 therefore focuses on the ensemble average, but also incorporates the individual model  
15 simulations to highlight uncertainties in the model projections. We also evaluate the  
16 sensitivity of the ensemble average model by sequential removal of the most poorly  
17 performing models over the mid-Atlantic region (Fig 2b). The change in mean model  
18 error is not monotonic (Fig 2b). While removing poorly performing models does  
19 generally come with an increase in mean model performance until the 13<sup>th</sup> model is  
20 removed, the improvement after the first few removals is minimal. The error increases  
21 sharply as more models are removed. Interestingly, the largest reduction in mean model  
22 error does not necessarily come from elimination of the most poorly performing models,

1 indicating that the uncorrelated model error is not necessarily a function of total model  
2 performance. However, rather than removing models which give the best reduction in  
3 mean model error (getting the right answer for the wrong reasons), we remove the worst  
4 performing models in order of their error score. Ultimately only two models (Models 15,  
5 6) are judged to influence the mean model error score sufficiently to justify the removal  
6 of additional degrees of freedom.

7  
8 This model subset is then averaged over the Chesapeake Bay watershed region to  
9 estimate changes in future climate. Mean model anomalies are calculated as the average  
10 of the individual model anomalies. Each individual model anomaly is referenced to its  
11 own monthly climatology calculated over the 1979-1999 time period following the  
12 guidelines for the IPCC AR4 report. Sea level height variability in the Mid-Atlantic Bight  
13 is also used to set a boundary condition for Chesapeake Bay and coastal Maryland  
14 regional sea level changes based on thermosteric sea level variability. Because not all of  
15 the models reported information for all scenarios, or for all variables within a scenario,  
16 there is variability in the number of models used to estimate the mean model for each  
17 variable.

## 18 19 **2.2. Choice of Scenarios**

20 This analysis focuses on the SRES B1 and A2 scenarios. The ratio of global averaged  
21 temperature increase for the B1 and A2 scenarios is 0.69:1.17, and in many areas this  
22 ratio is maintained on a regionally averaged basis (Christensen et al. 2007). However,

1 other quantities of interest such as precipitation do not remain in this linear ratio, and so  
2 both scenarios are presented.

3

4 The scenarios differ in their estimation of how the global economy and response to  
5 climate change will differ. The cumulative and annual emissions associated with these  
6 scenarios are shown in Figure 3. While emissions for the two scenarios begin to diverge  
7 significantly around 2025, and decline in the B1 scenario by 2050, the cumulative  
8 emissions do not significantly diverge until 2050. Because the system has a long  
9 memory, the full effects of this divergence are not yet felt by 2100. Thus, in the model  
10 projections, there is often little difference between the A2 and B1 scenarios until 2100.  
11 For reference, the mean model global averaged warming in 2100 for the A2, and B1  
12 scenarios are 3.4°C, and 1.8°C respectively (IPCC, 2007).

13

14 While the IPCC premise is that each scenario is equally likely (IPCC, 2007) they can  
15 alternatively be viewed as representing the differences between proactive and reactive  
16 response to climate change. In this case, the A2 scenario represents a reactive approach,  
17 with increasing CO<sub>2</sub> emissions through the next century, while the B1 scenario is  
18 proactive and reverses the emissions trend by 2050.

19

### 20 **2.3. Confidence Estimates**

21

22 There has been a great deal of improvement in estimating confidence in model  
23 projections (see Christensen et al, 2007 for a review of recent efforts), these methods

1 generally rely on an ensemble of projections from each model for developing probability  
2 density functions. Even with such methods, the range of parameter space sampled is  
3 modest. Here, we use the range of projections of the models to bracket possible  
4 outcomes. It remains a strong possibility that the models fail to capture significant  
5 physical processes, such as drought and floods that will lead to climate signals outside the  
6 present range of model projections.

7  
8 For this study, uncertainty is reported based on two criteria. The first criterion indicates  
9 model consensus, or the number of models that have positive or negative trends  
10 consistent with the mean model. Consensus is labeled “high” when the 75<sup>th</sup> – 25<sup>th</sup>  
11 percentile range anomaly spread is of the same sign. Consensus is “moderate” when the  
12 range is predominantly of one sign, and “low” when the range brackets zero. The second  
13 criterion stems from the magnitude of the model errors in reproducing 20<sup>th</sup> century  
14 climate. For example, the models predict temperature well (see below), thus confidence  
15 in quantities relating to temperature is labeled “high”. In contrast, the models predict the  
16 regional hydrological cycle less reliably than temperature. Thus, we have “moderate”  
17 confidence in model quantities that stem from or depend on precipitation or snowfall. We  
18 also have less confidence in model projections of extreme or unlikely events, since these  
19 generally occur at spatial scales much smaller than the model grid. Thus we characterize  
20 confidence in these quantities as “moderate” for temperature and “low” for hydrological  
21 quantities.

### 22 23 **3. ANALYSIS**

### 1        **3.1. Thermal effects**

#### 2        **Surface Air Temperature:**

3        In general, the models simulate air temperature quite accurately over the 20<sup>th</sup> century,  
4        based on the metrics discussed below. All the models have high ( $r^2 > 0.95$ ) correlation  
5        with the observed data, indicating that the timing of the seasonal temperature cycle is  
6        well simulated. At low frequencies, the 10 year filtered models and data are much more  
7        poorly correlated (MM  $r^2 = 0.5$ ). Most of the models (15 out of 20) have a higher standard  
8        deviation than the data, however this error was generally less than 10% of the standard  
9        deviation in the data. In most cases the annual average temperature bias, or mean  
10       temperature error relative to data, is less than 2°C, with the exception of models 11,12  
11       and 15. The mean model is 0.9°C colder than the data and its standard deviation is  
12       0.005°C high relative to the observed timeseries (standard deviation = 8.6°C). Observed  
13       local trend in the UEA temperature data is .009°C/year over the 20<sup>th</sup> century (1979-1999  
14       averaged minus 1920-1900 averaged), and the mean model trend is considerably lower, at  
15       .0008°C/year.

16  
17       These errors are generally consistent with the analysis of (Randall et al. 2007) which  
18       indicate a 1°C cool bias in the mid Atlantic region using the same dataset. If the analysis  
19       is restricted to the late 20<sup>th</sup> century (1979-2000), then the local temperature error drops to  
20       0.6°C. It is likely that these differences do not reflect improvements in model skill, but  
21       rather variability in the models coupled with changes in the data set associated with the  
22       increase in temperature monitoring stations in the late 20<sup>th</sup> century. (Najjar et al.  
23       Submitted) find similar but slightly higher error (0.8°C cold bias) and a much larger

1 winter error associated with an ensemble of Third Assessment Report models. However  
2 we find little seasonal difference in model error (range 0.9 to 0.5°C, from spring to fall).  
3  
4 Projected changes in temperature over the Chesapeake Bay watershed are shown in  
5 Figure 4a and Table 3. As might be predicted based on Figure 3a, which shows  
6 cumulative CO<sub>2</sub> emissions, the temperature changes for the A2 and B1 scenarios do not  
7 begin to diverge from each other significantly until 2050. The ratio of the B1:A2 scenario  
8 temperatures follows the ratio of the B1:A2 atmospheric CO<sub>2</sub> concentration closely,  
9 explaining the acceleration in warming in the A2 scenario after 2050. Winter  
10 temperatures are projected to rise at a slower rate than summertime temperatures with  
11 almost a 1°C difference seasonally in the A2 scenario, however these seasonal  
12 differences are small relative to the annual average anomaly. Seasonal differences are  
13 more modest in the B1 case, but are consistent with the projection for the A2 scenario in  
14 2060 (when mean annual average temperatures matched the B1 2100 warming)  
15 suggesting that the intra-seasonal differences are a function of the mean annual  
16 temperature and are not lagged.  
17  
18 These projections (4.3°C; range 4.0-4.8°C for A2 in 2100; summarized in Table 3) do not  
19 differ significantly from the estimates of Najjar et al, 2008 (3.9-4.7°C temperature change  
20 in 2100 for the A2 scenario). They are slightly lower than the recent study by (Hayhoe et  
21 al. 2007). This is expected, because Hayhoe et al, 2007 averaged over an area that  
22 extended farther to the north, and in general the magnitude of the projected warming  
23 trend increases towards the north. Although the range of temperature estimates for the

1 individual scenarios can be quite large, there is general agreement on the sign of  
2 predicted changes, and on the relative warming among seasons, thus, there is high model  
3 consensus in the estimates.

4  
5 It is important to note that these average temperature changes do not reflect the variability  
6 that remains in the climate system. Figure 4b illustrates a single model temperature  
7 anomaly time series. Model 5 is selected here because it represents the standard deviation  
8 of temperature over the Chesapeake Bay watershed in the present day well, while also  
9 having a high correlation with observations. Clearly, individual months and even years  
10 may have significant cold anomalies in the century to come while the average  
11 temperature continues to warm, so no single cold or warm event may be directly  
12 attributed to anthropogenic effects.

13

#### 14 **Chesapeake Bay Temperature:**

15 Because climate models do not resolve the Chesapeake Bay estuary, we relate air  
16 temperature to water temperature statistically. Changes in surface air temperature are  
17 highly correlated with sea surface temperature (SST) in Chesapeake Bay (Preston 2004;  
18 Secor and Wingate 2008). This is physically intuitive, as the mean depth of Chesapeake  
19 Bay is less than 7 meters, with the majority less than 2 meters, thus there is much less  
20 thermal latency as compared to a deeper system with a similar amount of vertical mixing.  
21 The observations show a trend of increasing water temperature of  $0.22^{\circ}\text{C}$  per decade,  
22 with much of that increase over the past 30 years, consistent with increasing air  
23 temperatures. This amounts to a warming of  $1.6^{\circ}\text{C}$  over much of the Bay since 1940

1 (Secor and Wingate 2008). Here, we use the mean model air temperature ( $T_{air}$ ) integrated  
2 over a smaller domain to predict observed Chesapeake Bay water temperatures (SST;  
3 data from Chesapeake Bay Program segment CB4MH, mesohaline) using a simple linear  
4 autoregression (adjusted  $r^2 = 0.96$ ):

$$SST(t) = 0.82976 \times T_{air}(t) + 0.30168 \times T_{air}(t - 2) + 1.63802 \quad (2)$$

6  
7 Where  $(t - 2)$  indicates a two month lag. The model is trained over the period from 1940-  
8 2004. Differences between air and ocean temperature are modest, (see Table 3), but show  
9 some differences. Fall SST anomalies tend to be slightly higher than summer anomalies  
10 in contrast to air temperature. This reflects the thermal inertia in the Chesapeake Bay,  
11 which leads to later maximum temperatures.

### 13 3.2. Hydrological Effects

#### 14 **Precipitation:**

15 Processes that drive precipitation are sensitive to model spatial scale, topography, initial  
16 conditions, and turbulence parameterizations, along with other factors; each of these  
17 factors tend to be poorly represented in climate models because of the compromises  
18 between spatial resolution and long integration times. This is evident in the modeled  
19 annual cycle in precipitation. The mean model has a pronounced spring maximum, and  
20 seasonal amplitude of  $39\text{mm month}^{-1}$ , as compared with the observations which have  
21 lower seasonal amplitude ( $33\text{mm month}^{-1}$ ), and a maximum in July. This advance in  
22 annual phase in the models is consistent with the model ensemble from the IPCC Third

1 Assessment Report discussed in Najjar et al, 2008, however the errors in the amplitude of  
2 the seasonal cycle are greatly reduced in the CMIP3 dataset. Correlations at the seasonal  
3 timescale range from very high ( $r^2 = 0.99$ ) to negatively correlated, with the mean model  
4 correlation with observations having an  $r^2 = 0.65$ . There is some consistent precipitation  
5 bias, with 14 of 20 models having a positive bias overall and 10 of the 20 having more  
6 than 10% higher precipitation on average than the observations; the mean model bias is to  
7 13% higher precipitation on an annual basis. Many of the models underestimate both the  
8 full and decadal filtered standard deviation of the precipitation (16 and 11 of the 20  
9 respectively). Trends in both mean model and observations are very small, and not  
10 statistically significant.

11

12 Figure 5 (see also Table 4) illustrates the change in precipitation anomaly for the two  
13 scenarios over time. Here, the 25<sup>th</sup> and 75<sup>th</sup> percentile range precipitation anomalies over  
14 twenty year periods from the entire model ensemble are shown as error bars, rather than  
15 the range of projections at one time point. This is done to highlight trends in interannual  
16 variability in precipitation rather than the inter model spread. Projections of winter  
17 rainfall show the greatest change, with increases of 5% by 2025 projected for both  
18 scenarios, 6.6 to 6.8% increase by 2050, and further increases of 10.4 to 12.6% by 2090  
19 for the low (B1) and high (A2) emissions scenarios respectively. However there is a very  
20 wide band of uncertainty around these mean tendencies and increases of that scale do not  
21 approach the level of present year-to-year variability in winter precipitation. Unlike for  
22 temperature, the A2 and B1 scenarios cannot be distinguished from each other based on  
23 the overlap of the model averages (not shown) and in most seasons the sign of the change

1 is within the range of the error bars. However, no season is projected to experience a  
2 substantial decrease in mean precipitation. Spring, summer and fall precipitation  
3 anomalies are smaller and not significantly different from zero when the range of the  
4 models is considered.

5  
6 Clearly, the mean increase in winter precipitation is much smaller than the present day  
7 range of variability shown in the error bars. Thus, short-term present day analogues to the  
8 average changes projected for monthly mean precipitation exist. The lower error bar  
9 represents the change to be expected in the lower 25<sup>th</sup> percentile of rainfall, and indicates  
10 that little change in low rainfall months is projected. The upper error bars however show  
11 an increasing trend in the highest 25<sup>th</sup> percentile of rainy months for both the A2 and B1  
12 scenarios. Essentially, the range of possible monthly mean precipitation is increased, with  
13 the mean shifted slightly higher, and little change to the lower end of the spectrum. For a  
14 smaller region comprising mainly the state of Maryland, the highest monthly  
15 precipitations anomalies of more than 100 mm/month are present less than 1% of the time  
16 at present, 2.7% of the time in the 2100 B1 scenario, and 5% of the time in the 2100 A2  
17 scenario. This is similar to the results of Hayhoe et al, 2007 and Najjar et al, 2008?, who  
18 also found the greatest increases in precipitation are likely to occur in winter (40% and  
19 9%) with smaller changes in other seasons. Because of the combined poorer  
20 understanding of the hydrological cycle, and the degree to which model simulations of  
21 the hydrological cycle depend on high spatial resolution, there is low confidence in  
22 hydrological projections.

23

1 **Soil Moisture:**

2 Soil moisture is an integral component of the hydrological cycle, influencing the rates of  
3 evaporation, groundwater recharge, and runoff. It is also a critical factor determining the  
4 success of agriculture as it determines the likelihood of drought conditions in areas where  
5 irrigation is limited. Because soil moisture retains a memory of the hydrological cycle  
6 over longer timescales than the instantaneous precipitation and evaporation, it is a useful  
7 measure of the integrated effects of hydrological changes. However, representation of  
8 soil moisture depends on the accuracy of the representation of the lower atmosphere,  
9 precipitation, and land surface models. (Li et al. 2007) showed in comparisons of 20<sup>th</sup>  
10 century observed and modeled soil moisture for the CMIP3 archive that the seasonal  
11 cycle was well represented in Illinois by most models, though trends in soil moisture in  
12 Asia were not well represented due to a failure to represent changes in solar irradiance  
13 that resulted from anthropogenic changes in tropospheric pollutants (Robock and Li  
14 2006).

15  
16 Trends in soil moisture (Figure 6, see also Table 4) are relatively consistent across the  
17 model ensemble. By 2100, the 25<sup>th</sup> to 75<sup>th</sup> percentile range of annual average, summer  
18 and fall soil moisture anomalies are consistently negative. The greatest decreases are  
19 predicted for fall soil moisture in the B1 scenario. The 20<sup>th</sup> century seasonal amplitude  
20 for soil moisture is  $110 \text{ kg m}^{-2}$ , so the largest projected autumn changes are not quite 20%  
21 of the seasonal cycle. It is unusual that the B1 scenario has more extreme changes than  
22 the A2 scenario; however this may be due to changes in the net precipitation minus  
23 evaporation (not shown). Summer and fall precipitation minus evaporation anomalies are

1 more strongly negative in the B1 than A2 scenario due to reduced evaporation in  
2 summertime in the A2 scenario. The two scenarios are significantly different based on the  
3 range of the model ensemble. (Hall et al. 2008) attribute the large summertime  
4 intermodel standard deviation (see the large range of soil moisture in the Fall, Figure 6),  
5 to the snow albedo feedback. As snow cover decreases, much more solar radiation is  
6 absorbed, and this affects the water carrying capacity of the system and persists into  
7 summer and fall.

8

9 There is little trend in winter and spring soil moisture despite winter increases in  
10 precipitation minus evaporation anomalies, suggesting that the soil has reached carrying  
11 capacity and remaining precipitation is diverted into runoff. This has important  
12 implications for the fate of the increased winter precipitation. Increased winter runoff into  
13 streams and rivers when temperatures are cold and denitrifying metabolic activity is low  
14 may mean higher nutrient loading for Chesapeake Bay (Howarth et al. 2006). Overall,  
15 while there is low confidence in the magnitude of the soil moisture signal, the models  
16 have good consensus on the increased likelihood of summer and fall drying of soils.

17

### 18 **Snow and Ice:**

19 The Chesapeake Bay itself is located at the southern edge of where significant snow  
20 accumulation occurs in winter. Its watershed, however, extends into a small portion of  
21 southern New York State. Significant storage of winter precipitation as snow and ice  
22 occurs in the watershed and the spring freshet of the Susquehanna River, the major  
23 tributary to Chesapeake Bay, is driven by this snow and ice storage (Najjar 1999). Miller

1 et al. (2006) further illustrated the sensitivity of spring discharge to winter weather  
2 patterns, explaining 54% of the variance in the spring freshet based on winter sea level  
3 pressure patterns. Climate models tend to poorly represent snow in general, and in  
4 particular snow melt, in part because they fail to represent the relationships between  
5 albedo and climate (Hall and Qu 2006).

6

7 Snow volume volume anomalies are expected to be negative under both climate scenarios  
8 (Figure 7). In the recent Northeast Climate Impacts assessment (Hayhoe et al. 2007),  
9 reductions in snow accumulation and earlier melt were also projected. The greatest  
10 changes occur in winter over this region, whereas the spring and fall seasons see little  
11 snow accumulation. Winter snow volume is 50<sup>th</sup> of its 20<sup>th</sup> century value by 2100 in both  
12 scenarios, suggesting that temperature and not precipitation which shows little change, is  
13 the dominant control on snow volume. Greater fractional changes occur in spring and  
14 fall, with fall snow volume reduced by more than 75% by 2025, then remaining  
15 unchanged until 2100. This is primarily associated with the loss of rare snowfalls in fall,  
16 rather than a change in average depth. Spring snow volume anomalies follow a more  
17 linear trend, decreasing to 75% of their current volume by 2100 in both scenarios.

18 Although confidence in modeled snow is low, there is a consensus among models on the  
19 direction of the change to be expected and this is in agreement with the tight relationship  
20 between temperature and snowpack.

21

22 Chesapeake Bay exhibits ice cover in nearshore environments during most years. On an  
23 irregular decadal basis, this ice cover extends across the upper bay creating a navigational

1 hazard in the mid-Bay channel. An ice-covered bay is also an event with cultural  
2 significance for many who live near Chesapeake Bay and recall skating or walking on the  
3 ice. Here cold events are defined relative to ice formation by averaging daily average  
4 temperatures over a 7 day period. The probability of a cold event is then calculated for  
5 the present day and for the high and low emissions scenarios in 2100, and the resulting  
6 probabilities are shown in Figure 8. The figure demonstrates how frequently an event that  
7 occurs every 1, 2, 5 and 10 years in the present day model ensemble would occur in the  
8 high and low emissions scenarios. If we estimate that mid-Bay freezing events occur  
9 every 10 years at present, then this frequency drops to every 25 to 40 years for the low  
10 and high emissions scenarios respectively.

11

### 12 3.3. Extreme and Synoptic Events

#### 13 Winds and Turbulent Kinetic Energy Inputs

14 Analysis of data collected in the second half of the twentieth century shows a general  
15 poleward shift in the average latitude of northern hemisphere extratropical cyclones. The  
16 poleward shift is accompanied by a decrease in frequency and an increase in  
17 intensity(Mccabe et al. 2001). Experiments with general circulation models illustrate  
18 similar changes associated with increasing greenhouse gas concentrations, and relate  
19 these shifts predominantly to changes in the meridional atmospheric temperature gradient  
20 (Yin 2005). Of particular interest in Chesapeake Bay, are changes to the frequency and  
21 intensity of Nor'Easters, which are low pressure systems that form off the coast of North  
22 Carolina and feed off the strong temperature gradient between the Labrador current and  
23 the Gulf Stream (Zielinski 2002). These storms are associated with cold temperatures,

1 high precipitation, and, often, elevated sea level and wave action that causes coastal  
2 erosion. There have been few studies that systematically evaluate the ability of a range of  
3 models to simulate storm frequency, intensity and path. (Bengtsson et al. 2005) used a  
4 single model (ECHAM5) and found a decrease in frequency and an increase in intensity  
5 of winter extratropical storms in the mid-Atlantic region. A similar trend was found in a  
6 regional climate model forced with the CGCM global model (Jiang and Perrie 2007). At  
7 present, there is little consensus however on how winter storminess in the mid-Atlantic  
8 may change in the next hundred years. This is also the case for summer tropical storms.  
9 There is substantial and active debate regarding tropical hurricane intensity, frequency,  
10 and relationships to climate change vs. natural variability (e.g. (Bengtsson et al. 2007;  
11 Elsner 2007; Emanuel 2005; Holland and Webster 2007; Jiang and Perrie 2007; Landsea  
12 et al. 2006). The net effects of storms and associated effects on mixing, erosion and sea  
13 level on Chesapeake Bay are therefore very difficult to predict currently.

14

15 Chesapeake Bay is highly stratified in summertime, and high nutrient inputs in spring  
16 accompanied by intensive mid-Bay recycling of organic matter often lead to hypoxia  
17 below the thermocline in the deeper channels of the Bay (Hagy et al. 2004). The degree  
18 of hypoxia has been shown to be related to the magnitude of spring freshwater discharge,  
19 although not all of the variability can be explained by nutrient inputs (Hagy et al. 2004).  
20 The degree of summertime stratification and the number of summertime events that mix  
21 through the water column oxygenating the deep waters also influences the intensity and  
22 areal extent of hypoxia (Roman et al. 2005). Mixing events are often associated with  
23 synoptic scale variability such as hurricanes or frontal passages. Although these events

1 are not well simulated in the climate models, here we evaluate whether there are changes  
2 in summertime wind speed associated with climate change scenarios.

3  
4 Probability distributions for daily wind speed over the state of Maryland during winter  
5 and summer seasons show no significant change between the 20<sup>th</sup> century, and the A2 or  
6 B1 projections for the year 2100 (not shown). This suggests that at the spatial resolution  
7 of the coupled climate models, no change in kinetic energy inputs to the Chesapeake Bay  
8 is projected.

9

#### 10 **Hydrological and Thermal Event Forcing:**

11 The information on monthly mean temperature and precipitation give an indication of  
12 generally warmer climate with wetter winters, however they do not reveal what changes  
13 to the frequency or intensity of synoptic events are projected to occur. However, because  
14 event scale forcing can play a dominant role in driving the ecosystem dynamics of  
15 Chesapeake Bay, we provide the bulk model projections relevant to assessing drought,  
16 flood, and heat wave events. Easterling et al. (1999), highlighted the difficulties in  
17 obtaining adequate datasets for validation of model predictions of extreme events.

18 Recently, a global database of some extreme event indices has been constructed for the  
19 second half of the twentieth century (Alexander et al. 2006). Here we present an index of  
20 extreme heat, metrics for short and long term drought, and for rainfall intensity.

21

#### 22 **Heat Waves:**

1 Figure 9a shows the average duration for the longest heat wave in a given year, calculated  
2 as the longest period with consecutive days above the 95<sup>th</sup> percentile daily maximum  
3 temperature for the 1961-1990 period. The index is averaged over twenty year periods,  
4 and over the model ensemble. Like monthly mean temperature, the A2 and B1 scenarios  
5 diverge only after 2050, following the cumulative CO<sub>2</sub> emissions. Both scenarios predict  
6 longer periods of extreme heat, with the A2 scenario predicting the greatest increases,  
7 from 8 days in the late 20<sup>th</sup> century, to as many as 85 consecutive days in 2100 (Table 5).  
8 Both scenarios suggest a doubling of average heat wave duration by 2025.

9

10 The annual probability of a various heat waves occurring is shown in Figure 8b. The  
11 histograms are calculated using all the models in the ensemble, then normalized. In the  
12 twentieth century, the probability distribution is one sided, with a high probability that  
13 heat waves will persist for less than 20 days. The B1 scenario shifts the average duration  
14 to longer periods, and flattens out the distribution. In the A1 scenario however, the  
15 probabilities are nearly equal that a given year will have a heat wave persisting for less  
16 than 20 days or for longer than 140 days (Fig 8b). Confidence in extreme events is lower  
17 than for the average temperature, thus confidence in the heat wave estimates is moderate.

18

19 Because Chesapeake Bay temperatures follow air temperature, but including a  
20 contribution from a two month lag due to thermal inertia, we can expect that the longer a  
21 heat wave persists, the more likely that SST, in particular temperatures in the shallow  
22 portions of the bay, will increase following the air temperature. Thus, more extended heat  
23 waves will create stronger thermal variations in bay temperature.

1

2 **Dry Periods:**

3 One measure of short-term or agricultural drought is the number of consecutive days  
4 without measurable rainfall. The Alexander et al. (2007) observationally derived database  
5 suggests that in the late twentieth century, the average number of consecutive dry days in  
6 the Chesapeake Bay watershed region was 14.5 days, and the mean model average is 15  
7 days. Figure 10a (see also Table 5) shows mean model consecutive dry days, and the  
8 probability that a given year will have a short-term period of drought. Only the A2  
9 scenario shows an increase in the number of consecutive dry days in 2100 from 15 to 17  
10 days, and most of this increase is projected for the latter half of the century. The  
11 probability distribution (Figure 9b) is also flattened in the A2 scenario, indicating that  
12 more variability in the number of short-term dry periods can be expected. Short-term  
13 drought increases may lead to increased water demand for crop irrigation. Although the  
14 model compares well with observations, confidence in these projections depends on the  
15 hydrological cycle, and is low.

16

17 **Long term Drought:**

18 Long term or water supply drought is affected by low precipitation periods that extend  
19 over multiple months. This is particularly important during the winter and spring when  
20 soil moisture, water tables and reservoir levels would normally experience recharge. To  
21 estimate this long-term drought probability, we average monthly mean precipitation  
22 anomalies over a two year period. Figure 11 illustrates the probability distribution of the  
23 two year averaged observed and modeled anomaly. These data are obtained over

1 relatively short intervals (20 years for each model, and 40 years of data) and thus do not  
2 reflect rare drought events (e.g. 40 to 100 year events), but rather infrequent events.  
3 Drought, where a rainfall deficit of greater than 30 cm is maintained over a two year  
4 period, occurs slightly more than 7% and 4% of the time at present in observations and  
5 models respectively (Figure 11). This probability changes slightly under the A2 and B1  
6 scenarios, however the models do not predict a likely increase in the incidence of long-  
7 term drought. In contrast, we can also examine precipitation excesses that persist over a  
8 period of two years or more. The models suggest that two-year precipitation excesses of  
9 more than 30 cm, which are observed less than 3% of the time in the data but do occur  
10 4% of the time in the 20<sup>th</sup> century models, will occur much more frequently in the future.  
11 The A2 and B1 scenarios have 30 cm excesses in precipitation occurring 33% and 18%  
12 of the time respectively at the end of the century. Thus, the models predict that while  
13 some moderate increase in short term drought may occur, the region is more likely to  
14 experience precipitation excesses in the long term. However, confidence in these  
15 predictions is low, and further efforts to simulate extreme events at a regional scale are  
16 needed to reduce uncertainty.

17

### 18 **Flood/Heavy Precipitation:**

19 Figure 12a (Table 5) shows the fraction of precipitation in a given year that occurs in  
20 events that could be classified as extreme according to present day conditions (events  
21 stronger than 95% of the rainfall events from 1960-1990). The Alexander et al. (2007)  
22 dataset indicates that 15% of the total annual precipitation falls in extreme events over the  
23 Chesapeake region. The mean model predicts a greater quantity, 22% (Fig 12a). Both

1 emission scenarios project an increasing likelihood (Figure 12b) that a high (35 to more  
2 than 40%) percentage of rainfall in a given year will fall as strong events, with greatly  
3 reduced likelihood that a given year will not experience significant rainfall in heavy  
4 events. Thus a general tendency for higher rainfall in short bursts may be expected.  
5 Confidence in this projection follows the hydrological cycle.

6  
7 Not shown are model averages that project only small changes in the number of days  
8 with more than 10 mm (about four tenths of an inch) of precipitation, with a slight  
9 increase (decrease) under the B1 (A2) scenario by the end of the century. Five-day  
10 maximum precipitation (not shown) is projected to increase more consistently from  
11 approximately 8.4 cm presently to 9.4 cm with little difference between higher and lower  
12 emissions scenarios. The maximum one-day precipitation over a year, a decade and a  
13 century is projected to increase. However, at present, a watershed in Maryland for  
14 example, might experience a flood due to more than 20 cm of rain in a single day only  
15 once every 100 years. The climate models consider 6.3 cm of rain in a single day to be a  
16 100-year event. This is partly because the 6.3 cm of rain is spread evenly over more than  
17 38,000 km<sup>2</sup> in the model because of the broad representation of space, however it does  
18 indicate the need to investigate event driven precipitation more closely for management  
19 purposes. With greater event driven precipitation, higher erosion and nutrient runoff may  
20 be expected with greater overland runoff and less uptake into soil moisture. This will  
21 increase nutrient and sediment loading into the bay, and may exacerbate the trend  
22 towards low summertime oxygen in the mainstem of the bay.

23

1  
2  
3  
4  
5  
6  
7  
8  
9  
10  
11  
12  
13  
14  
15  
16  
17  
18  
19  
20  
21

### 3.4. Sea Level

The IPCC AR4 report estimates global sea level rise of 23-51 cm and 38-18 cm for the A2 and B1 scenarios respectively at the year 2100. It should be noted that these estimates are not highly certain because of discrepancies between observed sea level change from satellites compared with the tide gauge record (Lombard et al. 2005; Miller and Douglas 2004) and also because these estimates do not include the potential for accelerated melting of continental ice sheets (Rahmstorf 2007). Besides these global estimates, the models predict local changes in sea level associated with changes in ocean circulation and local thermosteric anomalies from regional heating and cooling of the ocean. For example, at present the Atlantic Ocean off the mouth of Chesapeake Bay is relatively lower than other regions of the North Atlantic because the water is cooler than the warm (high) Gulf Stream transport and Sargasso Sea water against which it is juxtaposed to the south. Changes in relative heating or freshening of the Labrador Sea versus the Sargasso Sea, or in the position of the Gulf Stream may then affect the local sea level off the Mid-Atlantic. Landerer et al., (2007) analyze sea level anomaly relative to the global mean in the ECHAM5/MPI-OM model for the A1B (emissions midway between A2 and B1) scenario. They show that increases in local sea level anomaly relative to the global signal in the mid-Atlantic region reflect the poleward migration of the North Atlantic Current.

To evaluate the potential for local changes across a suite of models for the A2 and B1 scenarios, global average sea level is removed from each model at each time step, and

1 these projected sea level anomalies are differenced with the present day sea level  
2 anomaly (Figure 13). Although the CMIP3 ensemble has a lot of variability associated  
3 with regional sea level patterns, seven of the nine models we included show an increase  
4 in sea level anomaly, and three of the nine had a large anomaly, greater than 10 cm. This  
5 term should be added to the global averaged sea level rise for the A2 and B1 scenarios.  
6 Chesapeake Bay is also subject to crustal subsidence of  $1.5\text{mm y}^{-1}$  (Douglas 1991;  
7 Hohldahl and Morrison 1974) leading to a subsidence of 15 cm by 2100. If the global  
8 averaged sea level rise is added to local subsidence and the regional change in sea level,  
9 Chesapeake Bay could experience sea level rise of order 41-73 cm and 37-15 cm by 2100  
10 for scenarios A2 and B1. Maps of regions at particular risk for sea level rise are shown in  
11 (Titus and Richman 2001), or on the Environmental Protection Agency website.

12

13 Because of the large uncertainties in sea level rise as a result of accelerating loss of ice in  
14 Greenland and Antarctic ice sheets, confidence in the sea level projections is low.

15 However as a lower bound on possible sea level rise, confidence is high.

16

### 17 **3.5. Salinity:**

18 Model derived variables are used in a multiple linear autoregression to predict observed  
19 and projected Chesapeake Bay salinity. This relationship is much weaker than for  
20 temperature (adjusted  $r^2=0.39$ ), but significant ( $p\text{value}<2.2\text{e-}16$ ). The model uses soil

$$SSS(t) = -88340 \times pr(t) - 75010 \times pr(t-1) - 0.006625 \times mr(t) - 0.02833 \times mr(t-2) + 35.2 \quad (3)$$

21 moisture ( $mr$ ) and precipitation ( $pr$ ), adding other variables such as evaporation or

1 temperature was found to reduce the adjusted  $r^2$  values. Interestingly, this leads to  
2 differences in the sign of the salinity change in response to surface atmospheric forcing  
3 between the A2 and B1 scenarios (Figure 14). This occurs because the reduction in soil  
4 moisture is generally greater in the B1 scenario (see section 3.2).

5  
6 A global study of the effect of changing land use and its impact on dam impacted vs. free  
7 flowing rivers used the A2 scenario and the HadCM3 model to estimate changes in  
8 discharge (Palmer et al. 2008). This study suggests increases in river discharge for the  
9 Potomac and Susquehanna Rivers of 22 and 23% respectively by 2050. Observed runoff  
10 has increased in the Mid-Atlantic region since 1970, consistent with these trends (Lins  
11 and Slack 2005). If the relationship between precipitation and discharge is linear, we can  
12 extrapolate this from 3:22 precipitation:streamflow % increases in 2050 to 5:37  
13 precipitation:streamflow % increases in 2100 using the annual mean precipitation change  
14 in the mean model. Based on the analysis of (Gibson and Najjar 2000), this would  
15 translate to a salinity decrease in mid-Bay of 1.8. This change is much larger than the A2  
16 salinity change calculated from our empirical regression (-0.8), in part because the soil  
17 moisture and precipitation anomalies are not linear over time, so that the model  
18 projections flatten out after 2025.

19  
20 A previous study, (Hilton et al. 2008) suggests that increasing sea level 0.7-1.6 m by  
21 2100 leads to increases in mid-Bay salinity of 1.4-3.2 as a result of greater intrusion of  
22 salt water. Although sea level estimates are highly uncertain, all the models predict  
23 increases, thus some positive contribution to salinity as a result of sea level may be

1 expected. Coupled with the changes in precipitation and soil moisture shown here, this  
2 would tend to suggest that salinity changes might be generally positive and in the range  
3 from 0.0-3.7. There is low confidence in this estimate however, and greater effort should  
4 be made to improve regional hydrological and climate model estimates of discharge and  
5 salinity.

6

#### 7 **4. CONCLUSIONS**

8 The model projections paint a picture of a future Chesapeake Bay climate that is wetter,  
9 with more of the precipitation coming in winter in heavy rainfall events, rather than snow  
10 and thus resulting in less snow pack. This suggests the potential for increases in erosion,  
11 overland flows, and nutrient runoff. One mitigating factor may be a 20-40 day increase in  
12 growing season length (not shown), which could lead to more winter precipitation being  
13 absorbed by plants and forests. The projected changes over the next century lie well  
14 within the range of present day interannual variability. Temperature projections suggest a  
15 climate that is warmer in all seasons and has intensive heat waves throughout much of the  
16 summertime. Projected temperature changes (2.5-4.5°C) surpass the standard deviation of  
17 winter and summertime temperature over the past 50 years (winter: 1.57, summer:  
18 0.65°C). Thus, while interannual or decadal variability in precipitation provides a model  
19 for estuarine physical and ecological response to future climate perturbations, the changes  
20 projected for temperature are outside the bounds of what is observed at present. One  
21 potential indicator of the resiliency of an estuarine system to climate change effects, is to  
22 evaluate projected changes in the context of the magnitude of present day variability.

23

1 An important result of this study is the variability in seasonal response to climate change.  
2 Temperature and precipitation effects are not linear, and so the effects on bay physics and  
3 ecosystems may not be straightforward to predict. For example, Figure 4b suggests that  
4 month long cool periods close to the anomalies experienced today may still occur in the  
5 context of much warmer average temperatures. In general, this analysis, while limited in  
6 its ability to address extreme or event forcing, does suggest a more variable future  
7 climate, with a not only a broader seasonal range in temperature in Chesapeake Bay, but  
8 also increasing year to year variability in temperature and precipitation.

9

10 Stratification is set primarily by salinity in Chesapeake Bay, however thermal  
11 stratification may become more important, or may contribute to stronger stratification in  
12 summer and fall. Higher surface temperatures will exacerbate low oxygen conditions  
13 through both stratification increases that inhibit air-sea exchange and through temperature  
14 mediated oxygen solubility decrease. Rising sea level is projected to increase salinity,  
15 though there may be a competing surface salinity decrease as a result of increasing winter  
16 streamflow. These processes would further intensify the bay stratification, which may  
17 protect the sub pycnocline waters from some of the thermal excursions associated with  
18 heat waves. Combined, these factors would be projected to intensify summertime anoxia  
19 and hypoxia as projected by (Boesch et al. 2007).

20

21 For most of the variables analyzed, changes do not become significantly different from  
22 the initial conditions until 2100, based on error bars derived from the 25<sup>th</sup> and 75<sup>th</sup>  
23 percentile spread of the models. However, there are some aspects of climate that appear

1 to have rather steep initial trajectories. In particular, winter precipitation and response in  
2 precipitation minus evaporation change quite rapidly by 2025, and even level off in the  
3 case of precipitation minus evaporation. Local sea level changes resulting from changing  
4 circulation patterns are projected to change by nearly 3 cm by 2025 in addition to the  
5 global sea level change. Temperature, and snow pack show significant changes by 2025  
6 that are echoed in summertime soil moisture. This suggests that mitigation and adaptation  
7 strategies need to factor both short and long term change into their policies.

8

9 It should be emphasized that the confidence in model projections are estimates only, as  
10 the models have not been evaluated against observations for the range of greenhouse gas  
11 forcing employed in the A2 and B1 future projections. In fact, these projections  
12 themselves are only estimates of a range of possible futures. Efforts to build policies to  
13 counteract or to mitigate the effects of climate forcing in the Chesapeake Bay region need  
14 therefore to have strategies or feedbacks developed from the outset to evaluate and adapt  
15 planning as new information on climate change becomes available.

16

17 **ACKNOWLEDGEMENTS:** We acknowledge the modeling groups, the PCMDI and the  
18 WCRP's Working Group on Coupled Modelling for their roles in making available the  
19 WCRP CMIP3 multi-model dataset. Support of this dataset is provided by the Office of  
20 Science, U.S. Department of Energy. CDAT (Climate Data Analysis Tools from the  
21 Program for Climate Model Diagnosis and Intercomparison, Lawrence Livermore  
22 National Laboratory) was used for model analysis in this study. K. Smith, D. Boesch, and  
23 the members of the Maryland Commission on Climate Change Science and Technical

1 Working Group all contributed to the development of this study. The work was supported  
2 by NOAA's Climate Program Office, and by the Town Creek and Keith Campbell  
3 Foundations.

4

5 REFERENCES:

6

- 7 Alexander, L. V. and others 2006. Global observed changes in daily climate extremes of  
8 temperature and precipitation. *Journal of Geophysical Research-Atmospheres*  
9 **111**.
- 10 Bengtsson, L. and others 2007. How may tropical cyclones change in a warmer climate?  
11 *Tellus Series a-Dynamic Meteorology and Oceanography* **59**: 539-561.
- 12 Bengtsson, L., K. I. Hodges, and E. Roeckner. 2005. Storm Tracks and Climate Change.  
13 *Journal of Climate* **19**: 3518-3543.
- 14 Boesch, D. F., V. J. Coles, D. G. Kimmel, and W. D. Miller. 2007. Ramifications of  
15 climate change to Chesapeake Bay hypoxia. *Pew Environmental Series*.
- 16 Christensen, J. H. and others 2007. *Regional Climate Projections*. Cambridge University  
17 Press.
- 18 Collins, W. D. and others 2006. The Community Climate System Model Version 3  
19 (CCSM3). *Journal of Climate* **19**: 2122-2143.
- 20 Crane, R. G., and B. C. Hewitson. 1998. Doubled CO<sub>2</sub> precipitation changes for the  
21 susquehanna basin: Down-scaling from the genesis general circulation model.  
22 *International Journal of Climatology* **18**: 65-76.
- 23 Delworth, T. 2006. Preface to the Special Section. *Journal of Climate* **19**: 641.
- 24 Developers, K.-M. 2004. K-1 Coupled GCM (MIROC) Description, p. 28. *In* H. Hasumi  
25 and S. Emori [eds.], K-1 Technical Report No. 1. Center for Climate System  
26 Research (CCSR), University of Tokyo; National Institute for Environmental  
27 Studies (NIES); Frontier Research Center for Global Change (FRCGC)
- 28 Diansky, N. A., A. V. Bagnò, and V. B. Zalesny. 2002. Sigma model of global ocean  
29 circulation and its sensitivity to variations in wind stress. *Izv. Atmos. Ocean.*  
30 *Phys. (Engl. Transl.)* **38**: 477-494.
- 31 Diansky, N. A., and E. M. Volodin. 2002. Simulation of present-day climate with a  
32 coupled Atmosphere-ocean general circulation model. *Izv. Atmos. Ocean. Phys.*  
33 *(Engl. Transl.)* **38**: 732-747.
- 34 Douglas, B. C. 1991. Global sea level rise. *Journal of Geophysical Research* **96**: 6981-  
35 6992.
- 36 Elsner, J. B. 2007. Granger causality and Atlantic hurricanes. *Tellus Series a-Dynamic*  
37 *Meteorology and Oceanography* **59**: 476-485.
- 38 Emanuel, K. 2005. Increasing destructiveness of tropical cyclones over the past 30 years.  
39 *Nature* **436**: 686-688.
- 40 Flato, G. M. and others 2000. The Canadian Centre for Climate Modeling and Analysis  
41 Global Coupled Model and its Climate. *Climate Dynamics* **16**: 451-467.

- 1 Furevik, T., M. Bentsen, H. Drange, I. K. T. Kindem, N. G. Kvamsto, and A. Sorteberg.  
2 2003. Description and evaluation of the bergen climate model: ARPEGE coupled  
3 with MICOM. *Climate Dynamics* **21**: 27-51.
- 4 Gibson, J. R., and R. G. Najjar. 2000. The response of Chesapeake Bay salinity to  
5 climate-induced changes in streamflow. *Limnology and Oceanography* **45**: 1764-  
6 1772.
- 7 Giorgetta, M. A., G. P. Brasseur, E. Roeckner, and J. Marotzke. 2006. Preface to Special  
8 Section on Climate Models at the Max Planck Institute for Meteorology. *Journal*  
9 *of Climate* **19**: 3769-3770.
- 10 Gordon, C. and others 2000. The simulation of SST, sea ice extents and ocean heat  
11 transports in a version of the Hadley Centre coupled model without flux  
12 adjustments. *Clim. Dyn.* **16**: 147-168.
- 13 Gordon, H. B. and others 2002. The CSIRO Mk3 Climate System Model p. 130pp.  
14 Aspendale: CSIRO Atmospheric Research. (CSIRO Atmospheric Research  
15 technical paper; no. 60).
- 16 Gualdi, S., E. Scoccimarro, A. Bellucci, A. Grezio, E. Manzini, and A. Navarra. The  
17 INGV-SXG coupled General Circulation Model.  
18 <https://www.cmcc.it/web/public/ANS/models/ingv-sxg>
- 19 Hagy, J. D., W. R. Boynton, C. W. Keefe, and K. V. Wood. 2004. Hypoxia in  
20 Chesapeake Bay, 1950-2001: Long-term change in relation to nutrient loading  
21 and river flow. *Estuaries* **27**: 634-658.
- 22 Hall, A., X. Qu, and J. D. Neelin. 2008. Improving predictions of summer climate change  
23 in the United States. *Geophysical Research Letters* **35**.
- 24 Hayhoe, K. and others 2007. Past and future changes in climate and hydrological  
25 indicators in the US Northeast. *Climate Dynamics* **28**: 381-407.
- 26 Hilton, T. W., R. G. Najjar, L. Zhong, and M. Li. 2008. , Is there a signal of sea-level rise  
27 in Chesapeake Bay salinity? *J. Geophys. Res.* **Submitted**.
- 28 Hohldahl, S. R., and N. L. Morrison. 1974. Regional investigations of vertical crustal  
29 movements in the U.S. using precise relevelings and maregraph data  
30 . *Tectonophysics* **23**: 373-390.
- 31 Holland, G. J., and P. J. Webster. 2007. Heightened tropical cyclone activity in the North  
32 Atlantic: natural variability or climate trend? *Philosophical Transactions of the*  
33 *Royal Society a-Mathematical Physical and Engineering Sciences* **365**: 2695-  
34 2716.
- 35 Howarth, R. W., D. P. Swaney, E. W. Boyer, R. Marino, N. Jaworski, and C. Goodale.  
36 2006. The influence of climate on average nitrogen export from large watersheds  
37 in the Northeastern United States. *Biogeochemistry* **79**: 163-186.
- 38 Hulme, M. 1992. A 1951-80 global land precipitation climatology for the evaluation of  
39 general-circulation models *Climate Dynamics* **7**: 57-72.
- 40 ---. 1994. Validation of large-scale precipitation fields in General Circulation Models.  
41 NATO ASI Series, Springer-Verlag.
- 42 Jiang, J., and W. Perrie. 2007. The impacts of climate change on autumn North Atlantic  
43 midlatitude cyclones. *Journal of Climate* **20**: 1174-1187.
- 44 Johns, T. C. and others 2006. The new Hadley Centre climate model HadGEM1:  
45 Evaluation of coupled simulations. *J. Climate* **19**: 1327-1353.

- 1 Landsea, C. W., B. A. Harper, K. Hoarau, and J. A. Knaff. 2006. Can we detect trends in  
2 extreme tropical cyclones? *Science* **313**: 452-454.
- 3 Legutke, S., and R. Voss. 1999. The Hamburg Atmosphere-Ocean Coupled Circulation  
4 Model E C H O-G. *In* D. Modellberatungsgruppe [ed.], Technical Report No. 18.  
5 Max Planck Institute for Meteorology
- 6 Li, H. B., A. Robock, and M. Wild. 2007. Evaluation of Intergovernmental Panel on  
7 Climate Change Fourth Assessment soil moisture simulations for the second half  
8 of the twentieth century. *Journal of Geophysical Research-Atmospheres* **112**.
- 9 Lins, H. R., and J. R. Slack. 2005. Streamflow trends in the United States, p. 4pp. *In* U. S.  
10 G. S. F. S. 2005-3017 [ed.].
- 11 Lombard, A., C. A., K. Dominh, C. C., and R. S. Nerem. 2005. Thermosteric sea level  
12 rise for the past 50 years; comparison with  
13 tide gauges and inference on water mass contribution. *Global and Planetary Change* **48**:  
14 303-312.
- 15 Lucarini, L., and G. L. Russell. 2002. Comparison of mean climate trends in the northern  
16 hemisphere between National Centers for Environmental Prediction and two  
17 atmosphere-ocean model forced runs. *Journal of Geophysical Research* **107**.
- 18 Marti, O. and others 2005. The new IPSL climate system model: IPSL-CM4.  
19 Institut Pierre Simon Laplace.
- 20 McCabe, G. J., M. P. Clark, and M. C. Serreze. 2001. Trends in Northern Hemisphere  
21 surface cyclone frequency and intensity. *J. Climate* **14**: 2763-2768.
- 22 Meehl, G. A. and others 2007. *Global Climate Projections*. Cambridge University Press.
- 23 Miller, L., and B. C. Douglas. 2004. Mass and volume contributions to twentieth-century  
24 global sea level rise. *Nature* **428**: 406-409.
- 25 Najjar, R., L. Patterson, and S. Graham. Submitted. Climate simulations of major Mid-  
26 Atlantic watersheds. *Estuaries*?
- 27 New, M., D. Lister, M. Hulme, and I. Makin. 2002. A high-resolution data set of surface  
28 climate over global land areas. *Climate Research* **21**: 1-25.
- 29 Palmer, M. A. and others 2008. Climate change and the world's river basins:  
30 anticipating management options. *Frontiers in Ecology and the Environment* **6**: 81-89.
- 31 Pope, V., M. L. Gallani, P. R. Rowntree, and R. A. Stratton. 2000. The impact of new  
32 physical parameterizations in the Hadley Centre climate model: HadAM3. *Clim.*  
33 *Dyn.* **16**: 123-146.
- 34 Preston, B. L. 2004. Observed winter warming of the Chesapeake Bay estuary (1949-  
35 2002): Implications for ecosystem management. *Environmental Management* **34**:  
36 125-139.
- 37 Rahmstorf, S. 2007. A Semi-Empirical Approach to Projecting Future Sea-Level Rise.  
38 *Science* **315**: 368-370.
- 39 Randall, D. A. and others [eds.]. 2007. *Climate Models and Their Evaluation*. Cambridge  
40 University Press.
- 41 Reichler, T., and J. Kim. 2008. How well do coupled models simulate today's climate?  
42 *Bulletin of the American Meteorological Society* **In Press**.
- 43 Robock, A., and H. B. Li. 2006. Solar dimming and CO2 effects on soil moisture trends.  
44 *Geophysical Research Letters* **33**.
- 45 Roman, M. R. and others 2005. Chesapeake

1 Bay plankton and fish abundance enhanced by Hurricane Isabel. EOS Transactions **86**:  
2 261-265.

3 Russell, G. L., J. R. Miller, and D. Rind. 1995. A coupled atmosphere-ocean model for  
4 transient climate change studies. Atmosphere-ocean **33**: 683-730.

5 Salas-Méla, D. 2002. A global coupled sea ice-ocean model. Ocean Modelling **4**: 137-  
6 172.

7 Schmidt, G. A. and others 2005. Present day atmospheric simulations using GISS  
8 ModelE: Comparison to in-situ, satellite and reanalysis data. Journal of Climate  
9 **19**: 153-192.

10 Secor, D. H., and R. L. Wingate. 2008. A 69 year record of warming in the Chesapeake  
11 Bay. In Preparation.

12 Titus, J. G., and C. Richman. 2001. Maps of Lands Vulnerable to Sea Level Rise:  
13 Modeled Elevations along the U.S. Atlantic and Gulf Coasts Climate Research.  
14 Washington, W. M. and others 2000. Parallel climate model (PCM) control and transient  
15 simulations. Clim. Dyn. **16**: 755-774.

16 Wilby, R. L., S. P. Charles, E. Zorita, B. Timbal, P. Whetton, and L. O. Mearns. 2004.  
17 Guidelines for Use of Climate Scenarios Developed from Statistical Downscaling  
18 Methods, p. 27pp., Task Group on Data and Scenario Support for Impacts and  
19 Climate Analysis. Intergovernmental Panel on Climate Change.

20 Yin, J. H. 2005. A Consistent Poleward Shift of the Storm Tracks in Simulations of 21st  
21 Century Climate. Geophysical Research Letters **32**.

22 Yongqiang, Y., Y. Rucong, Z. Xuehong, and L. Hailong. 2002. A flexible global coupled  
23 climate model. Adv. Atmos. Sci. **19**: 169-190.

24 Yongqiang, Y., Z. Xuehong, and Y. G. 2004. Global coupled ocean- atmosphere general  
25 circulation models in LASG/IAP. Adv. Atmos. Sci. **21**: 444-455.

26 Yukimoto, S. and others 2001. The New Meteorological Research Institute Coupled  
27 GCM (MRI-CGCM2) --- Model Climate and Variability --- Pap. Meteor. and  
28 Geophys. **51**: 47-88.

29  
30  
31

1 FIGURE LEGENDS:

2

3 Figure 1: Map of the regions used for averaging the global model output for this study

4 superimposed on surface air temperature for one of the models (20).

5

6 Figure 2a: Integrated model error for both precipitation and temperature metrics. The

7 mean model is shown to the left with the lowest error.

8

9 Figure 2b: The mean model error as a function of the number of models removed from

10 the average. Models are removed in the order of worst performing to best performing.

11

12 Figure 3: a) Cumulative carbon dioxide emissions for the 21<sup>st</sup> century in the A2 and B1

13 SRES scenarios. b) Annual carbon dioxide emissions for the A2 and B1 scenarios.

14

15 Figure 4: a) Surface air temperature anomaly for the Chesapeake Bay watershed. b)

16 Monthly surface air temperature anomaly for one of the climate models (#5), illustrating

17 the variability in temperature for the A2 and B1 scenarios.

18

19 Figure 5: Percent change in monthly mean precipitation relative to the 1979-2000 time

20 period annual cycle. Diamond symbols are used for the A2, and circles for the B1

21 scenario. Here, the vertical error bars indicate the spread in the model ensemble monthly

22 variability over a 20-year period centered on the data point. The upper and lower limits

23 represent the 25<sup>th</sup> upper and lower percentiles.

24

1 Figure 6: Change in soil moisture relative to the 1979-2000 time period. Error bars  
2 indicate the 25<sup>th</sup> and 75<sup>th</sup> percentile spread of the model ensemble.

3

4 Figure 7: Snow volume anomaly (m) based on snow depth multiplied by the fractional  
5 area of coverage.

6

7 Figure 8: Frequency of ice cover events in 2100. Ice spans the upper Chesapeake Bay at  
8 roughly decadal intervals at present. In the A2 scenario, this frequency might diminish to  
9 40-year intervals, or nearly 25-year intervals for the B2 scenario.

10

11 Figure 9: a) Mean model average duration of the longest heat wave in a given year for the  
12 A2 and B1 scenarios. b) Probability that a given year will have a heat wave persisting for  
13 the indicated periods.

14

15 Figure 10: a) Mean model average duration of the longest stretch of consecutive dry days  
16 in a given year for the A2 and B1 scenarios. b) probability that a given year will have a  
17 consecutive stretch of dry days lasting for the indicated periods.

18

19 Figure 11: Long-term drought probability based on two year averaged monthly rainfall  
20 over relatively short (20 year) time spans.

21

1 Figure 12: a) Percent of rainfall that falls as extreme events (greater than the 95<sup>th</sup>  
2 percentile over 1960-1990 for the A2 and B1 scenarios. b) probability that a given year  
3 will have more or less rainfall in extreme events.

4

5 Figure 13: Local sea level anomaly relative to a time varying global mean. Thus, the  
6 increase reflects a change in the pattern of sea level variation in the Atlantic relative to  
7 the global mean over time.

8

9 Figure 14: Predicted salinity anomaly based on the formula in equation 3.

10

11

12

Model ID	Sponsor(s), Country	Reference
1	BCCR-BCM2.0	Bjerknes Centre for Climate Research, Norway (Furevik et al. 2003)
2	CCSM3	National Center for Atmospheric Research, USA (Collins et al. 2006)
3	CGCM3.1(T47)	Canadian Centre for Climate Modelling and Analysis ,Canada (Flato et al. 2000)
4	CGCM3.1(T63)	Canadian Centre for Climate Modelling & Analysis, Canada (Flato et al. 2000)
5	CNRM-CM3	Météo-France/Centre National de Recherches Météorologiques, France (Salas-Méla 2002)
6	CSIRO-MK3.0	Commonwealth Scientific and Industrial Research Organization (CSIRO) Atmospheric Research, Australia (Gordon et al. 2002)
7	CSIRO-MK3.5	Commonwealth Scientific and Industrial Research Organization (CSIRO) Atmospheric Research, Australia (Gordon et al. 2002)
8	ECHAM5/MPI-OM	Max Planck Institute for Meteorology, Germany (Giorgetta et al. 2006)
9	ECHO-G	Meteorological Institute of the University of Bonn, Meteorological Research Institute of the Korea Meteorological Administration (KMA), and Model and Data Group, Germany/Korea (Legutke and Voss 1999)
10	FGOALS-g1.0	LASG / Institute of Atmospheric Physics, China (Yongqiang et al. 2002; Yongqiang et al. 2004)
11	GFDL-CM2.0	U.S. Department of Commerce/ National Oceanic and Atmospheric Administration (NOAA)/ Geophysical Fluid Dynamics Laboratory (GFDL), USA (Delworth 2006)
12	GFDL-CM2.1	U.S. Department of Commerce/ National Oceanic and Atmospheric Administration (NOAA)/ Geophysical Fluid Dynamics Laboratory (GFDL), USA (Delworth 2006)
13	GISS-AOM	National Aeronautics and Space Administration (NASA)/ Goddard Institute for Space Studies (GISS), USA (Lucarini and Russell 2002; Russell et al. 1995)
14	GISS-EH	National Aeronautics and Space Administration (NASA)/ Goddard Institute for Space Studies (GISS), USA (Schmidt et al. 2005)
15	GISS-ER	National Aeronautics and Space Administration (NASA)/ Goddard Institute for Space Studies (GISS), USA (Schmidt et al. 2005)
16	INGV-SXG	Instituto Nazionale di Geofisica e Vulcanologia, Italy (Gualdi et al. )
17	INM-CM3.0	Institute for Numerical Mathematics, Russia (Diansky et al. 2002; Diansky and Volodin 2002)
18	IPSL-CM4	Institut Pierre Simon Laplace, France (Marti et al. 2005)
19	MIROC3.2(hires)	Center for Climate System Research (The University of Tokyo), National Institute for Environmental Studies, and Frontier Research Center for Global Change (JAMSTEC), Japan (Developers 2004)
20	MIROC3.2(medres)	Center for Climate System Research (The University of Tokyo), National Institute for Environmental Studies, and Frontier Research Center for Global Change (JAMSTEC), Japan (Developers 2004)
21	MRI-CGCM2.3.2	Meteorological Research Institute, Japan (Yukimoto et al. 2001)
22	PCM	National Center for Atmospheric Research, USA (Washington et al. 2000)
23	UKMO-HadCM3	Hadley Centre for Climate Prediction and Research / Met Office, UK (Gordon et al. 2000; Pope et al. 2000)
24	UKMO-HadGEM1	Hadley Centre for Climate Prediction and Research / Met Office, UK (Johns et al. 2006)

Table 1: Models used in this study.

1  
2  
3

Error	Precipitation Weighting	Temperature Weighting
Model – data correlation	1.0	0.5
Filtered model – data correlation	1.0	1.0
Model – data mean absolute difference	0.5	0.5
Model – data mean difference	0.5	0.5
Model – data trend difference	1.0	1.0
Model – data standard deviation difference	1.0	1.0
Filtered model – data standard deviation difference	1.0	1.0

**Table 2:** Weights for the general error metric.

4  
5  
6  
7

1

Anomalies	2025		2050		2100	
	B1	A2	B1	A2	B1	A2
Annual surface air temperature	0.9<1.1<1.3	0.8<1.1<1.3	1.5<1.7<1.9	1.8<2.1<2.5	2.2<2.5<3.0	4.0<4.3<4.8
Winter surface air temperature	0.6<1.0<1.6	0.7<1.0<1.2	1.1<1.5<1.7	1.6<2.0<2.1	1.9<2.3<2.7	3.3<3.8<4.0
Spring surface air temperature	0.8<1.1<1.4	0.9<1.0<1.2	1.5<1.8<2.1	1.6<2.0<2.4	2.2<2.5<2.9	3.6<4.1<4.7
Summer surface air temperature	1.0<1.2<1.4	0.9<1.1<1.3	1.4<1.8<2.0	1.8<2.2<2.6	2.2<2.7<3.1	4.3<4.8<5.2
Fall surface air temperature	0.9<1.1<1.3	0.9<1.2<1.5	1.4<1.8<2.1	1.9<2.2<2.5	2.2<2.6<3.1	3.9<4.5<5.1
Annual sea surface temperature	1.0	1.0	1.7	2.2	2.5	4.7
Winter sea surface temperature	0.9	1.0	1.6	2.0	2.4	4.1
Spring sea surface temperature	1.0	0.9	1.6	2.0	2.5	4.3
Summer sea surface temperature	1.0	1.1	1.7	2.2	2.6	5.1
Fall sea surface temperature	1.0	1.2	1.8	2.3	2.6	5.1

**Table 3:** Air and Sea temperature anomalies relative to 1979-2000 for the A2 and B1 scenarios for three time periods. The ranges represent the 25<sup>th</sup>, mean, and 75<sup>th</sup> percentile ranges of the model ensembles. SST does not have a range of values, only the mean model was calculated.

2

3

1

Anomalies	2025		2050		2100	
	B1	A2	B1	A2	B1	A2
Annual precipitation	0.5<2.7<4.6	-0.5<2.8<5.4	0.8<3.6<6.2	-1.6<3.7<8.2	2.5<4.9<8.0	0<5.4<11.3
Winter precipitation	1.5<5.2<6.9	0.8<4.8<5.5	2.9<7.0<11.3	2.1<7.0<11.8	6.3<10.3<15.2	4.6<12.9<21.9
Spring precipitation	-3.5<1.9<6.5	0.9<1.0<1.2	-.7<2.8<5.6	-2.1<4.0<7.6	1.2<5.9<12.5	-1.2<4.5<10.0
Summer precipitation	-1.0<1.6<4.0	-1.9<1.7<4.4	-2.0<3.4<7.7	-3.4<1.2<3.6	-2.4<0.2<2.7	-1.2<1.6<7.9
Fall precipitation	-4.8<2.3<6.8	-1.6<2.0<5.3	-2.5<1.1<4.6	-2.9<2.8<4.7	0.0<3.7<9.5	-5.1<3.3<10.0
Annual soil moisture	-6.0<-1.7<1.3	-3.4<0.1<3.3	-7.9<-4.8<-0.6	-7.2<-4.4<1.2	-11.0<-10.9<-4.1	-9.8<-6.2<-2.2
Winter soil moisture	-3.3<0.6<4.2	-1.8<1.6<4.5	-4.8<-1.6<2.0	-8.2<-0.4<6.4	-6.6<-6.0<3.4	-2.2<0.2<4.9
Spring soil moisture	-6.9<-0.4<2.4	-3.4<1.1<6.0	-2.1<-0.1<2.9	-6.5<-3.4<1.4	-8.5<-5.5<1.5	-7.4<-2.6<2.6
Summer soil moisture	-8.34<-3.28<1.3	-6.1<-1.7<1.6	-11.4<-6.3<-.3	-13.1<-8.5<-.1	-16.9<-14.7<-7.1	-18.3<-11.7<-7.7
Fall soil moisture	-8.8<-3.9<-0.5	-5.2<-0.9<2.3	-18.33<-11.0<-6.6	-8.9<-5.1<2.5	-21.2<-17.2<-2.8	-21.4<-11.6<-5.7

**Table 4:** Precipitation percent, and soil moisture absolute anomalies relative to 1979-2000 for the A2 and B1 scenarios for three time periods. The ranges represent the 25<sup>th</sup>, mean, and 75<sup>th</sup> percentile ranges of the model ensembles.

2

3

1

Extreme Indices	2025		2050		2100	
	B1	A2	B1	A2	B1	A2
Heat wave duration (days)	9.0<16.2<23.1	8.7<15.1<22.1	11.0<22.5<31.7	12.3<27.1<40.4	15.2<35.5<50.1	53.5<85.4<119.2
Consecutive dry days (days)	13.2<14.5<15.6	13.2<14.6<15.8	13.5<15.3<16.4	15.0<15.6<16.7	14.1<15.5<16.6	16.7<17.0<17.7
Fraction of rainfall in intense events	21.1<23.3<24.9	22.8<23.4<23.8	22.3<24.1<26.2	23.6<25.1<26.6	25.2<26.6<28.4	24.3<26.0<27.2

**Table 5:** Extreme event indices calculated over the Chesapeake Bay watershed for the A2 and B1 scenarios for three time periods. The ranges represent the 25<sup>th</sup>, mean, and 75<sup>th</sup> percentile ranges of the model ensembles.

2

3

1  
2  
3

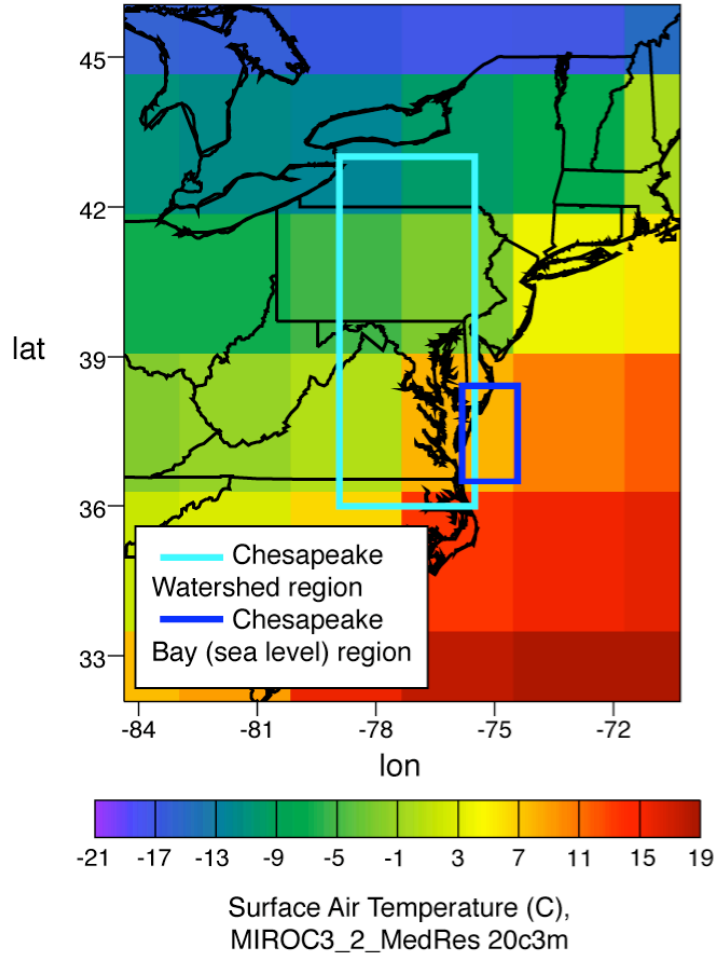


Figure 1: Map of the regions used for averaging the global model output for this study superimposed on surface air temperature for one of the models (20).

1  
2  
3  
4  
5  
6  
7  
8  
9  
10  
11  
12  
13

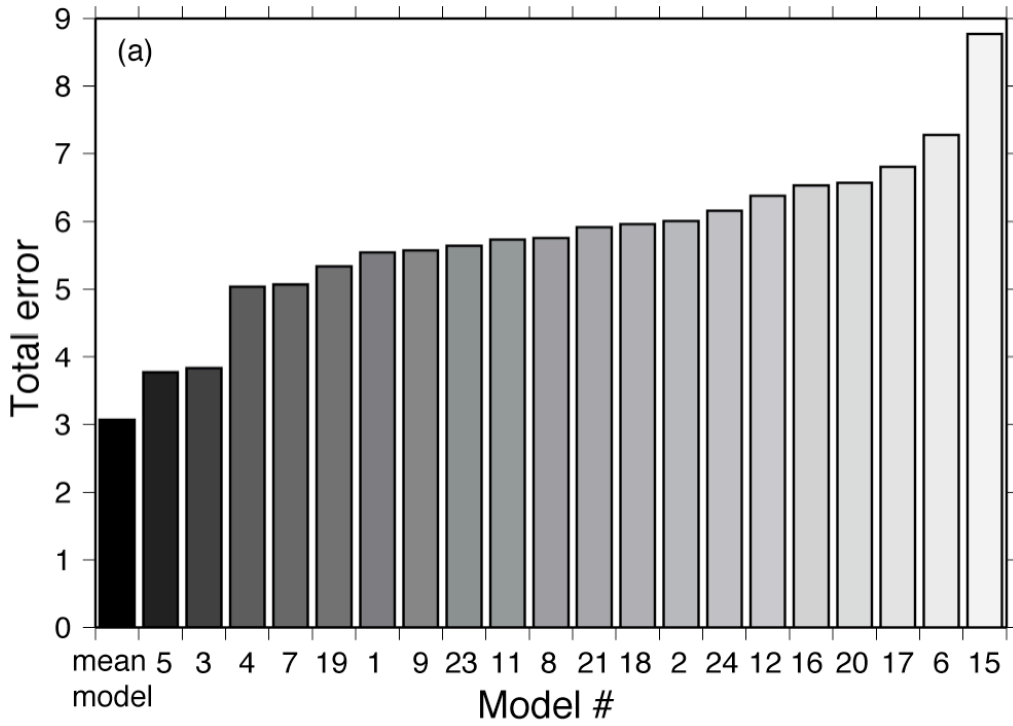


Figure 2a: Integrated model error for both precipitation and temperature metrics. The mean model is shown to the left with the lowest error.

1  
2  
3  
4  
5  
6  
7

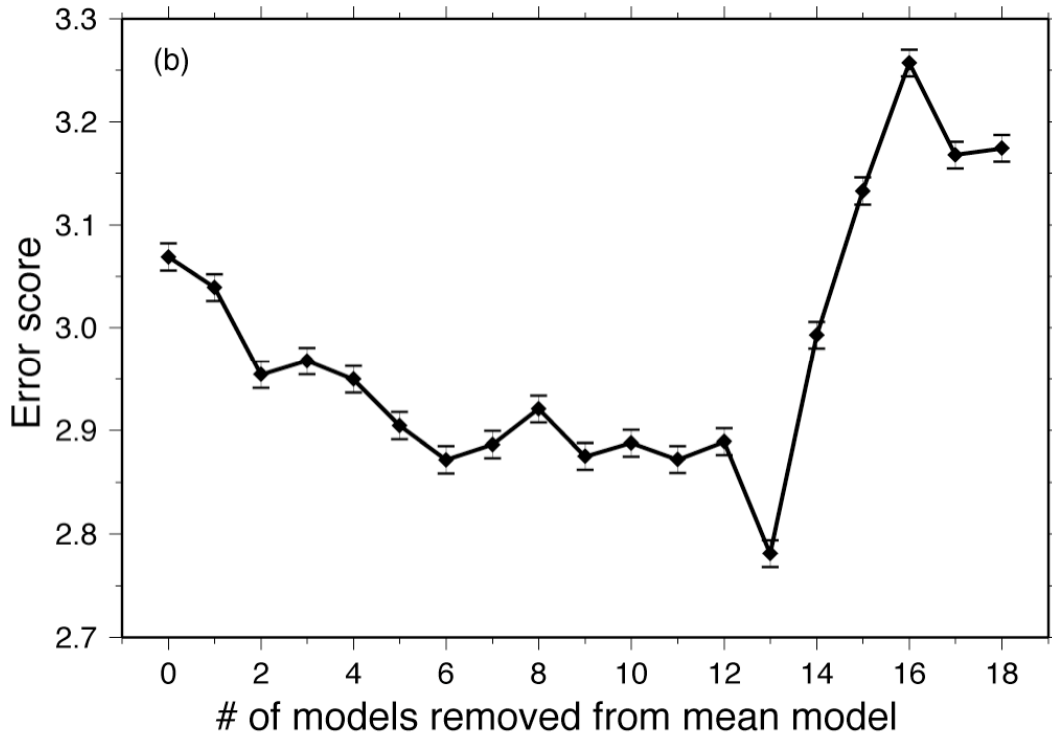


Figure 2b: The mean model error as a function of the number of models removed from the average. Models are removed in the order of worst performing to best performing.

1

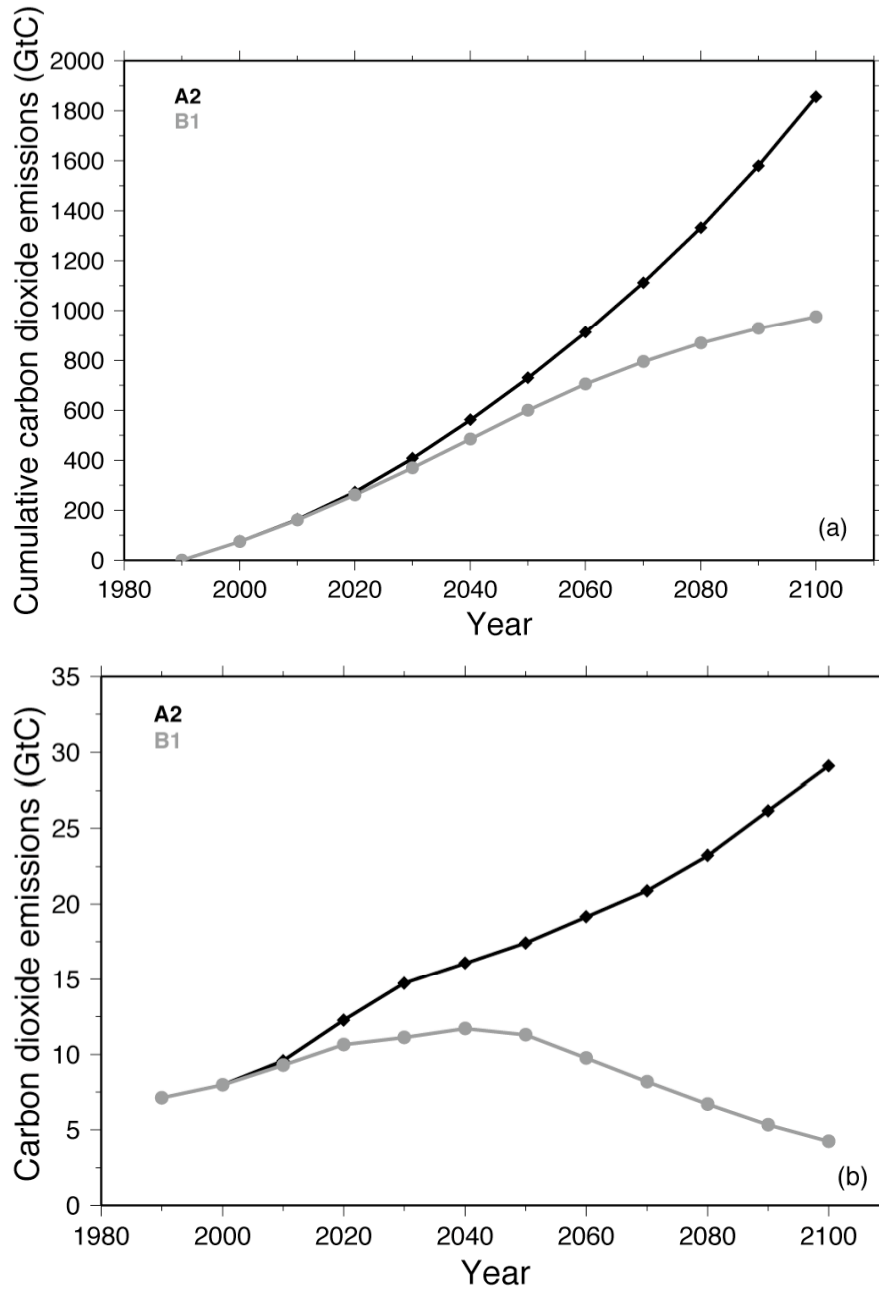


Figure 3: a) Cumulative carbon dioxide emissions for the 21<sup>st</sup> century in the A2 and B1 SRES scenarios. b) Annual carbon dioxide emissions for the A2 and B1 scenarios.

1  
2

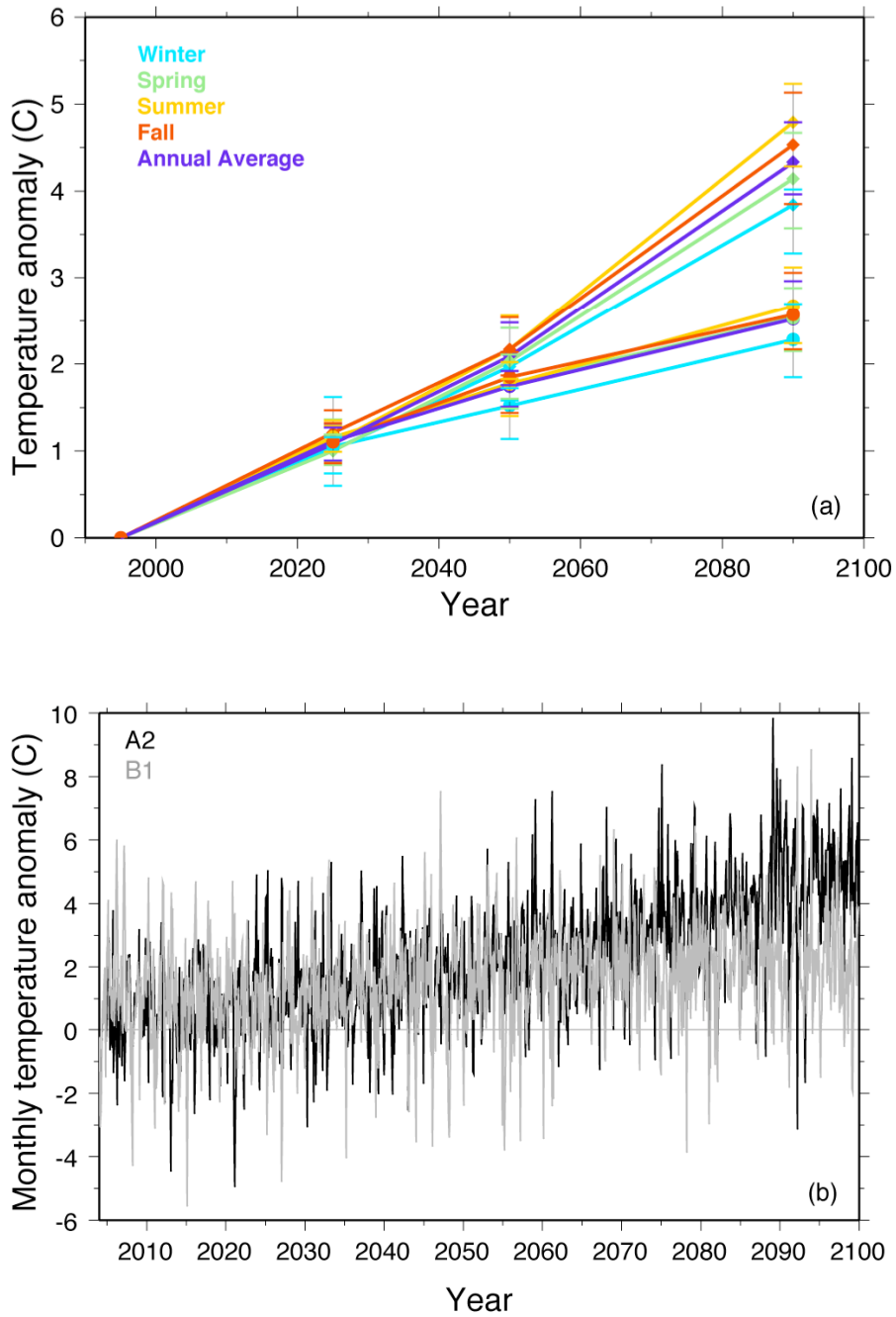


Figure 4: a) Surface air temperature anomaly for the Chesapeake Bay watershed. b) Monthly surface air temperature anomaly for one of the climate models (#5), illustrating the variability in temperature for the A2 and B1 scenarios.

## Precipitation Anomaly Variability

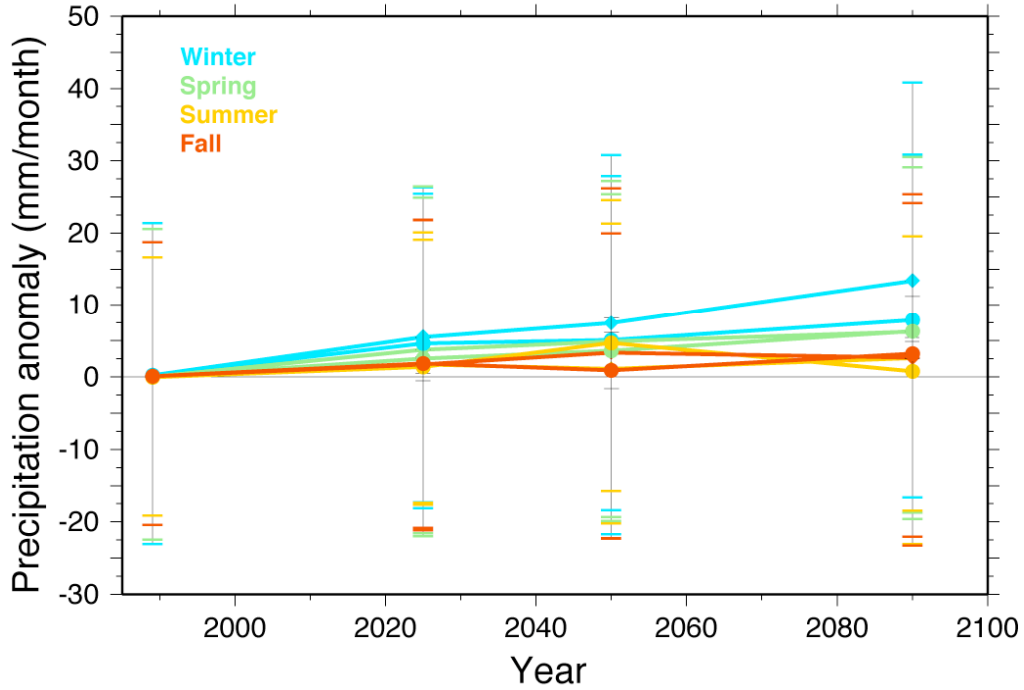


Figure 5: Percent change in monthly mean precipitation relative to the 1979-2000 time period annual cycle. Diamond symbols are used for the A2, and circles for the B1 scenario. Here, the vertical error bars indicate the spread in the model ensemble monthly variability over a 20-year period centered on the data point. The upper and lower limits represent the 25<sup>th</sup> upper and lower percentiles.

1  
2  
3

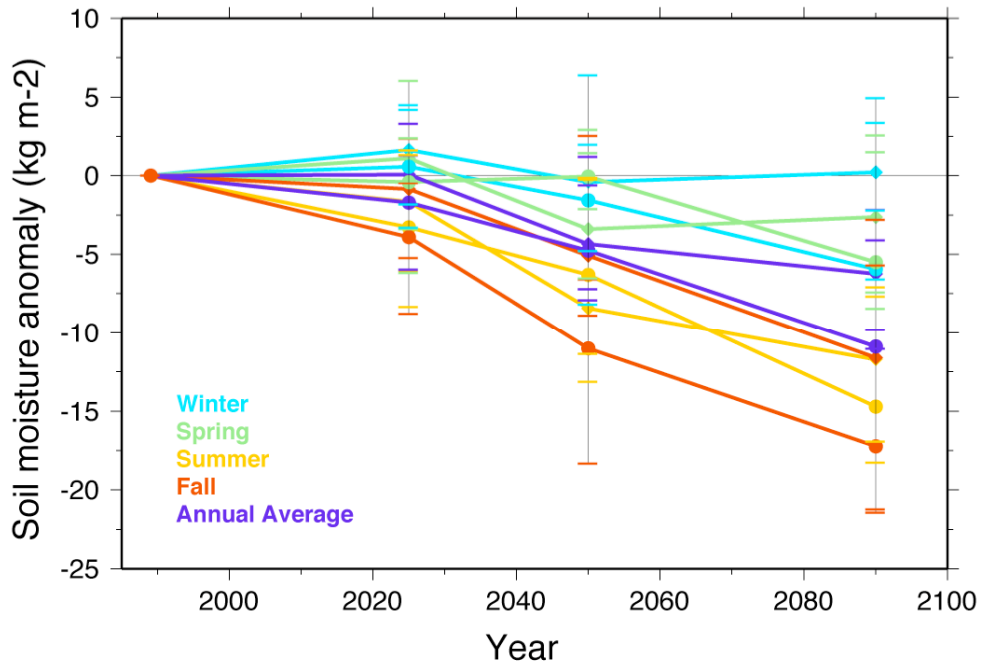


Figure 6: Change in soil moisture relative to the 1979-2000 time period. Error bars indicate the 25<sup>th</sup> and 75<sup>th</sup> percentile spread of the model ensemble.

1  
2  
3

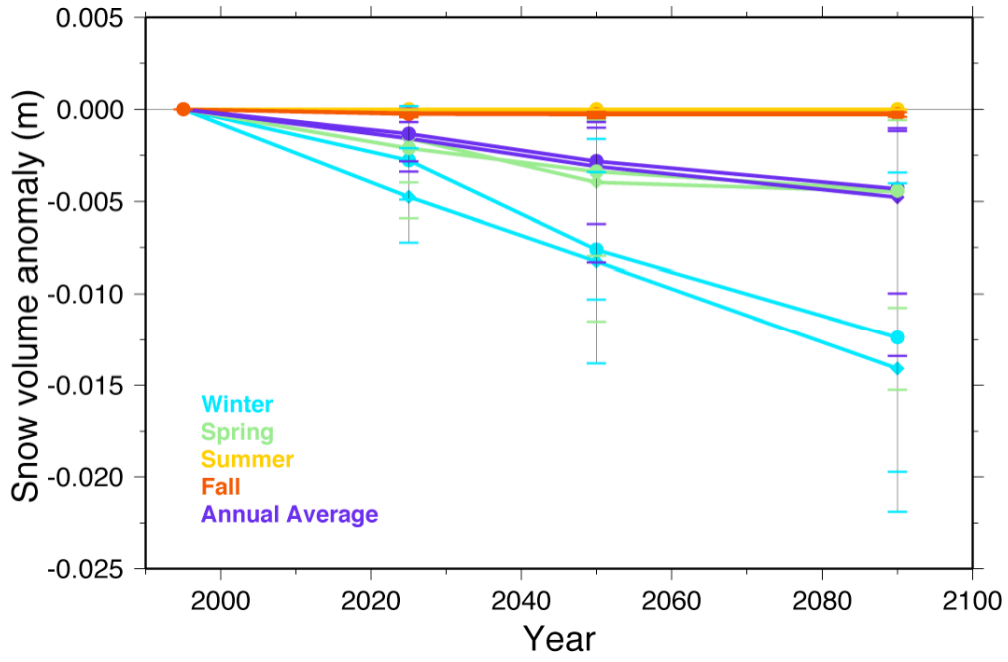


Figure 7: Snow volume anomaly (m) based on snow depth multiplied by the fractional area of coverage.

1  
2  
3  
4  
5  
6  
7  
8  
9  
10  
11  
12  
13  
14  
15  
16  
17  
18  
19  
20

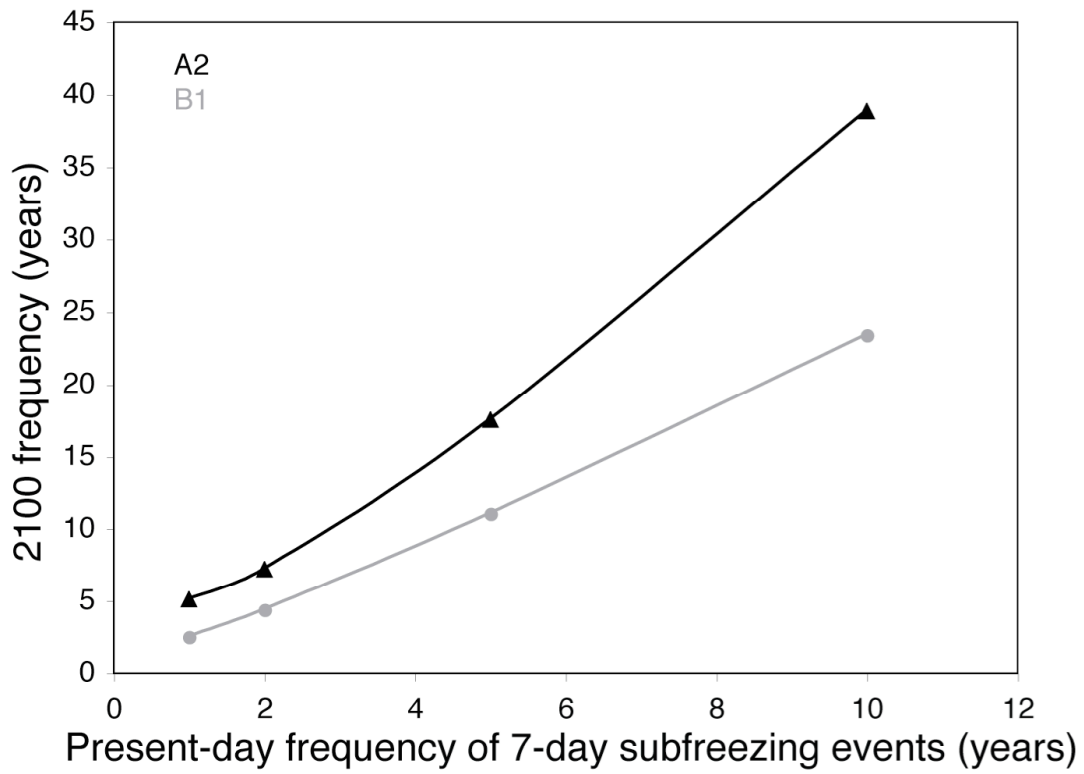


Figure 8: Frequency of ice cover events in 2100. Ice spans the upper Chesapeake Bay at roughly decadal intervals at present. In the A2 scenario, this frequency might diminish to 40-year intervals, or nearly 25-year intervals for the B2 scenario.

1  
2

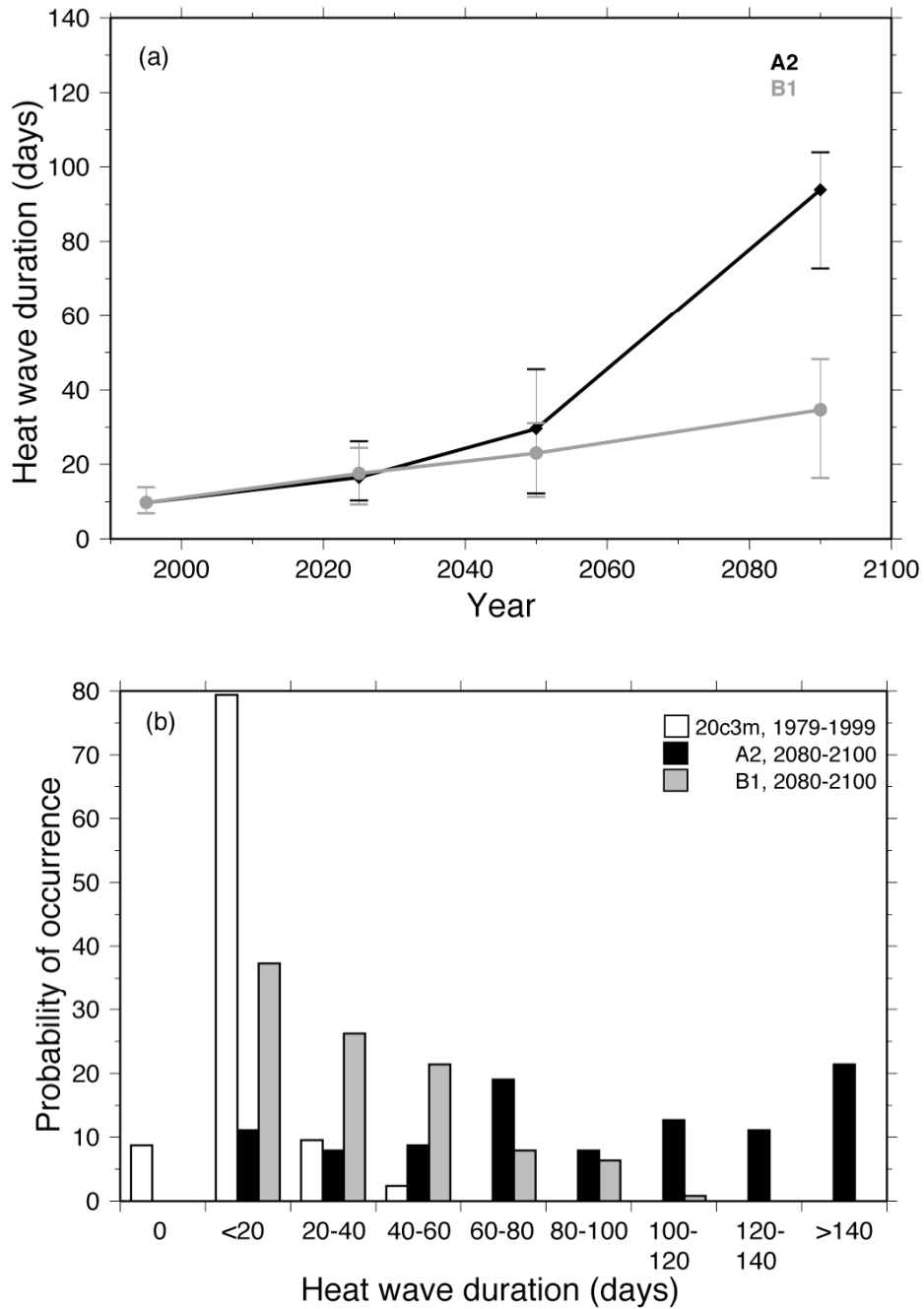


Figure 9: a) Mean model average duration of the longest heat wave in a given year for the A2 and B1 scenarios. b) Probability that a given year will have a heat wave persisting for the indicated periods.

1  
2  
3  
4  
5  
6  
7  
8

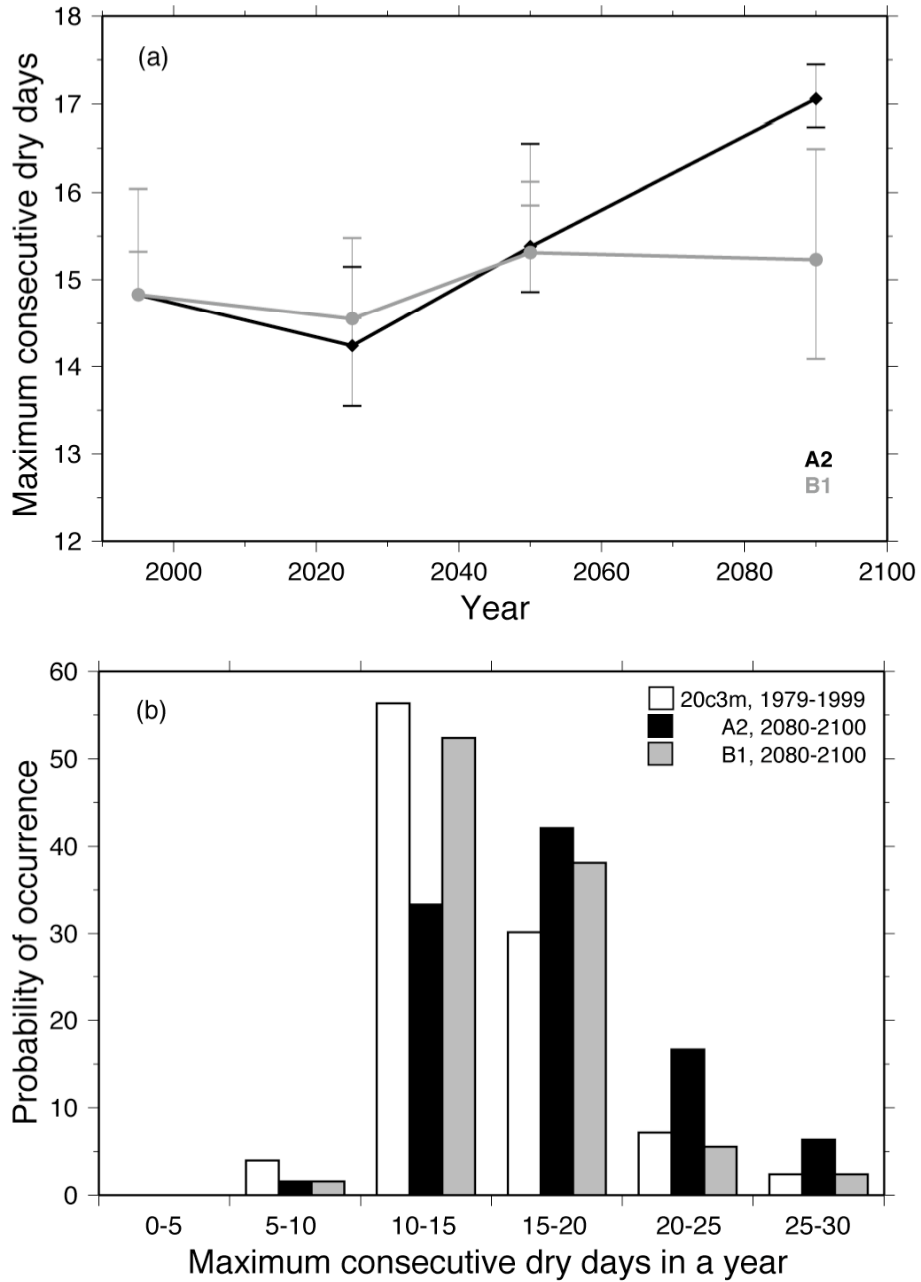


Figure 10: a) Mean model average duration of the longest stretch of consecutive dry days in a given year for the A2 and B1 scenarios. b) probability that a given year will have a consecutive stretch of dry days lasting for the indicated periods.

1

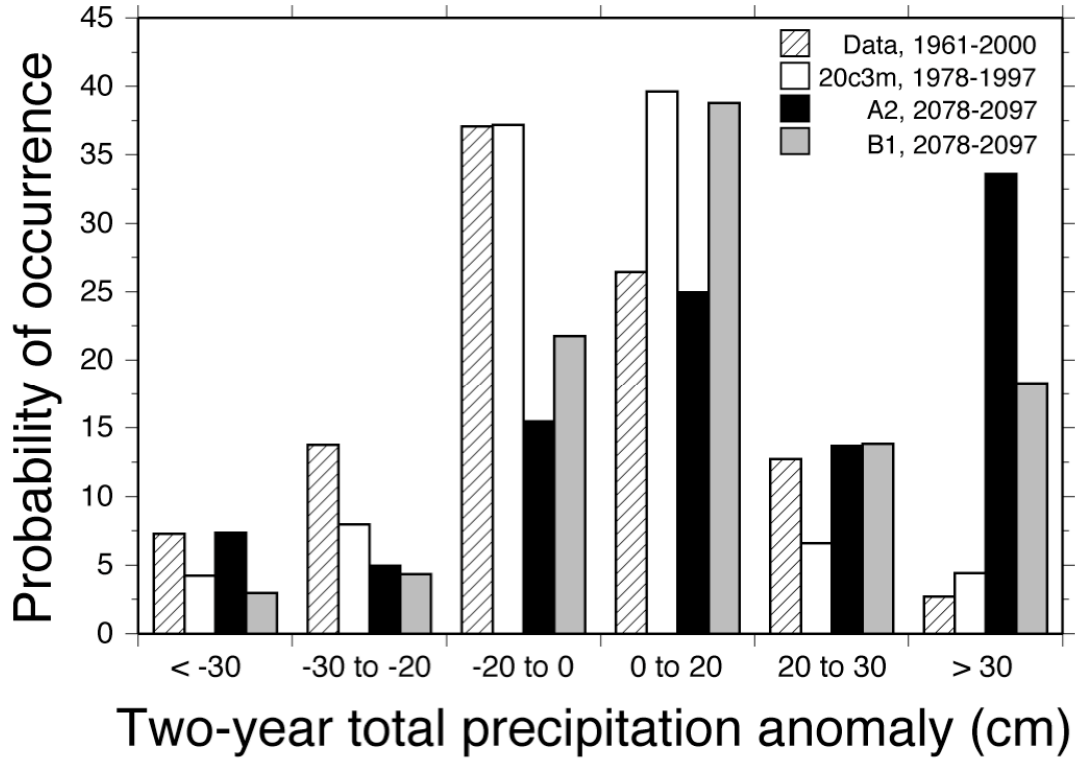


Figure 11: Long-term drought probability based on two year averaged monthly rainfall over relatively short (20 year) time spans.

1

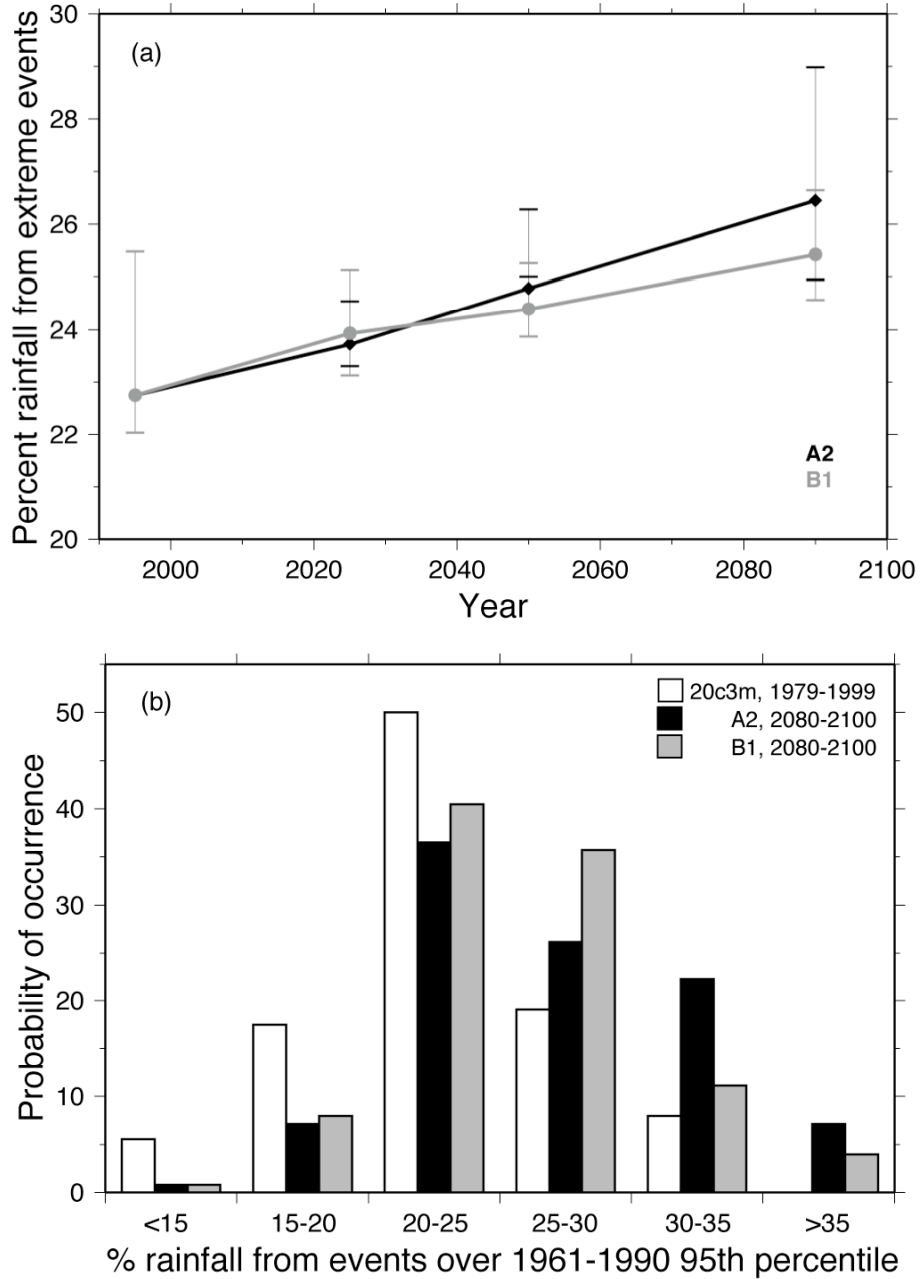


Figure 12: a) Percent of rainfall that falls as extreme events (greater than the 95<sup>th</sup> percentile over 1960-1990) for the A2 and B1 scenarios. b) probability that a given year will have more or less rainfall in extreme events.

1

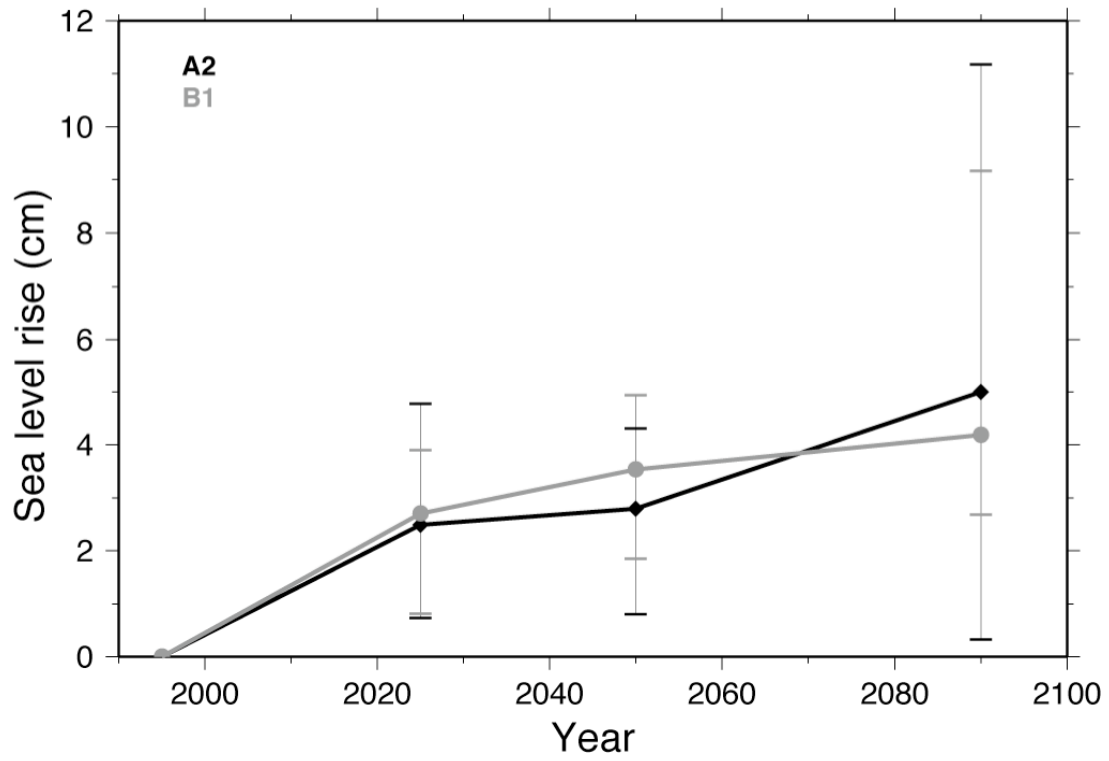


Figure 13: Local sea level anomaly relative to a time varying global mean. Thus, the increase reflects a change in the pattern of sea level variation in the Atlantic relative to the global mean over time.

1  
2

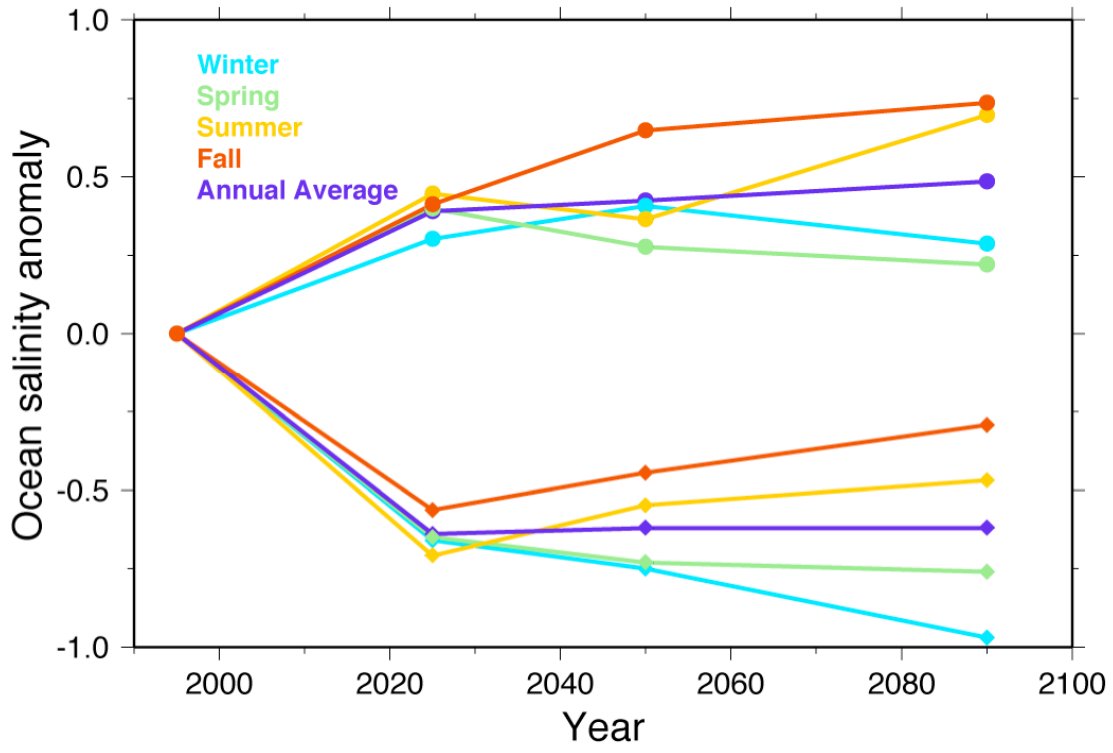


Figure 14: Predicted salinity anomaly based on the formula in equation 3.

